Particle radiation from relativistic plasmas contained by soliton waves

2009 J. Phys. A: Math. Theor. 42 105501

(http://iopscience.iop.org/1751-8121/42/10/105501)

IOP PUBLISHING JOURNAL OF PHYSICS A: MATHEMATICAL AND THEORETICAL

J. Phys. A: Math. Theor. **42** (2009) 105501 (35pp) doi:10.1088/1751-8113/42/10/105501

Particle radiation from relativistic plasmas contained by soliton waves

U Schaefer-Rolffs[1], I Lerche[2] and R C Tautz[3]

[1] Leibniz-Institut für Atmosphärenphysik, Universität Rostock, D-18225 Kühlungsborn, Germany
[2] Institut für Geowissenschaften, Naturwissenschaftliche Fakultät III, Martin-Luther-Universität Halle, D-06099 Halle, Germany
[3] Institut für Theoretische Physik, Lehrstuhl IV: Weltraum- und Astrophysik, Ruhr-Universität Bochum, D-44780 Bochum, Germany

E-mail: schaefer-rolffs@iap-kborn.de, lercheian@yahoo.com and rct@tp4.rub.de

Received 5 December 2008, in final form 13 January 2009
Published 11 February 2009
Online at stacks.iop.org/JPhysA/42/105501

Abstract

In the last few years, the Weibel instability has undergone a change from a marginal phenomenon to a more intense field of research especially in astrophysics. The possibility of magnetic field creation in an unmagnetized plasma enables new applications and the explanation of many scenarios that are still intensely debated. In a previous paper (Schaefer-Rolffs and Lerche 2006 *Phys. Plasmas* **13** 062303), the fundamentals of a nonlinear theory of solitary Weibel modes were derived. The main prerequisite is a bulk of charged particles moving conjoined in one direction, while perpendicular small fluctuations are possible. Such a constraint is obviously fulfilled in any relativistic astrophysical jet, e.g. in gamma-ray bursts or in the jets of active galactic nuclei. This paper provides calculations concerning the frequency spectra of radiation produced from relativistic electrons contained by such solitary waves. Furthermore, the influence of polarization and the Faraday effect are considered.

PACS numbers: 52.25.Dg, 52.27.Ny, 52.35.−g, 94.20.wf, 94.20.wj, 94.20.ws

1. Introduction

The enigma of gamma-ray bursts (GRBs) tasked astrophysicists since the first publication by Klebesadel *et al* in 1973 [1]. The fact that satellites detected the radiation only during a time of about 10 s did not allow further observations in other wavelength domains, and the identification of optical or radio counterparts was not possible. Thus, it was not even clear if the GRBs originated in our galaxy or in distant sources (see, e.g., [2]). It was only clear that the sources must be very compact because of the fast variation of the radiation. First hints of

the origin resulted from BATSE observations [3, 4] of the Compton Gamma-Ray Observatory in the mid-1990s. Although observation with other telescopes was still not possible, the large number of events and their isotropic distribution over the sky practically excluded an origin inside our galaxy [5]. However, early attempts to find GRB counterparts also failed [6, 7] until the first BeppoSAX results in 1997; the cameras allowed accurate positionings (of order several arc minutes) within a few hours, thereby allowing optical and radio telescopes to catch afterglows of the events [8, 9]. Red shift measurements then confirmed the host objects to be galaxies at cosmological distances [10, 11].

Independently from the specific progenitors, the observed brightness of the cosmological GRBs requires energies of about 10^{54} erg for isotropic emission from the source. In combination with the compactness of the GRBs, an $e^{\pm}, \gamma$ fireball, similar to a supernova explosion but with relativistic parameters, is favored as a model for the GRBs. The interaction with ambient material triggers shocks, which determine the observed power-law spectra of the afterglow. The most efficient processes for relativistic particles to lose energy are through synchrotron radiation—provided a magnetic field is present—and inverse Compton scattering. However, as of now the origin and mechanism of the required magnetic fields remain elusive [12].

The problem of the large amount of energy injected in a small volume can be ameliorated with the assumption of jet-like blast wave structures in GRBs. The total required energy is then reduced by the factor of the solid angle $\Omega/(4\pi)$ into which the blast waves are emitted. Due to the high pressure behind the shock the question of the stability of the jet becomes important, because the thermal velocity dispersion perpendicular to the jet flow can also be relativistic and so cannot be neglected in favor of only the parallel bulk velocity. However, another relativistic effect intervenes so that the jet flow can stay collimated. The jet cannot expand perpendicular to the jet axis faster than its internal speed of sound ($c/3^{1/2}$ in the ultrarelativistic limit). A detailed overview of the theory of GRBs is given in [13–16].

Here we investigate the radiation production of a GRB afterglow in electromagnetic soliton waves without the need for an ambient magnetic field. In a previous paper [17], we showed that self-consistent soliton waves can arise in a relativistic plasma and thus interact with electrons in the jet. In section 2, we give a short discussion of nonlinear waves in such plasmas with some astrophysical parameters. In section 3, we calculate the power and frequency spectrum of electron emission for a single electron and for a distribution of electrons. In section 4, we consider polarization and Faraday rotation related to the radiation. Finally, section 5 gives a short discussion and conclusion.

2. The soliton wave structure

Let

$$f_a(\varpi_x, \varpi_y, \varpi_z) \equiv \frac{F_a\left(\varpi_x, \varpi_y^2\right)\delta(\varpi_z)}{(m_a c)^2} \tag{1}$$

be a class of particle distribution functions, where ϖ_i are normalized momentum components and m_a is the rest mass of the particles a with $\varpi_x = p_x/(m_a c) + z_a A(\zeta)$, $\varpi_y = p_y/(m_a c)$ and $\varpi_z = \Gamma_L - \xi p_z/(m_a c)$, where p_a is the physical momentum, $A(\zeta)$ is the vector potential, $\zeta = Z - \xi ct$, the z-direction of the plasma moving with the constant (bulk) velocity $V_b = v_z = c/\xi$, $z_a = e_a/(m_a c^2)$ and $\Gamma_L = \left(1+\left(p_x^2+p_y^2+p_z^2\right)\big/(m_a c)^2\right)^{1/2}$. This behavior, with a constant flow speed c/ξ in the z-direction and an arbitrary distribution perpendicular to the z-direction, is a representation of jets in astrophysical plasmas, e.g. in GRBs or active galactic

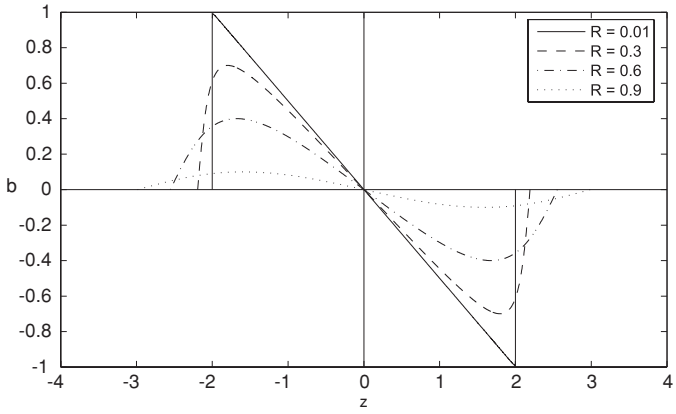

Figure 1. The normalized magnetic field $b(z)$ with varying R. The higher the R, the smaller is the maximum of b and the larger is $z_{\rm end}$ where the field vanishes. As $R \to 0$, corresponding to a large amplitude $A_{\rm max}$, the field steepens and the location of $z_{\rm max} = \zeta_{\rm max}/L$ approaches $z_{\rm end} = \zeta_{\rm end}/L$.

nuclei (AGNs). One can then find transverse electromagnetic soliton waves (as described in [17]) obeying the wave equation

$$\left(\frac{\partial A}{\partial \zeta}\right)^2 = \frac{8\pi}{(\xi^2-1)^{\frac{3}{2}}} \sum_a n_a m_a c^2 \int (E_\perp(A_{\rm max}, \varpi) - E_\perp(A, \varpi)) F_a \, {\rm d}\varpi_x \, {\rm d}\varpi_y, \tag{2}$$

where n_a and e_a are the number density and charge of the particle a, respectively, $E_\perp = \left[1 + \varpi_y^2 + (\varpi_x - z_a A)^2\right]^{1/2}$, the particle energy perpendicular to the z-axis, and $A_{\rm max}$ is the maximum value for the potential.

An analytical treatment of equation (2) can be given when $A_{\rm max}$ and A are both large yielding soliton waves [17] while, when A is small, equation (2) yields sinusoidal waves without a soliton behavior. Thus, a perturbation in the plasma may first cause aperiodic linear Weibel modes that can grow to become nonlinear soliton waves. With the normalized potential, $u = A/A_{\rm max}$, and magnetic field, $b = B/B_{\rm max}$, the solution of equation (2) for the magnetic field is given [17] as

$$b^2 = ({\rm d}u/{\rm d}z)^2 = (1-u)(u-R^2)/u, \tag{3}$$

where $B_{\rm max}^2 = ({\rm d}A/{\rm d}\zeta)_{\rm max}^2 = (1-R)^2 A_{\rm max}^2/L^2$, $R^2 = G_2/\left(2G_0 A_{\rm max}^2\right)$, $z = \zeta/L$ is the normalized length with $L^2 = (\xi^2-1)^{\frac{3}{2}} A_{\rm max}/G_0$ and

$$G_0 = 8\pi \sum_a n_a |e_a| \int {\rm d}^2\varpi \, F_a = 8\pi \sum_a n_a |e_a| > 0, \tag{4a}$$

$$G_2 = 8\pi \sum_a n_a |e_a| z_a^{-2} \int {\rm d}^2\varpi \, F_a \left(1 + \varpi_y^2\right) > 0. \tag{4b}$$

As shown in figure 1, the structure of the soliton wave depends only on the parameter R involving the zeroth and second moments of the distribution function and on the maximum potential. The crucial points are now the magnitude of the factor $A_{\rm max}$ and the particle density n_a. With $z_i = e/(Mc^2)$, it can be shown [17] that for a soliton wave to exist in an electron–proton plasma (with particle masses $m = \mu M$ and M for electrons and protons, respectively) one requires

$$(z_i A_{\rm max})^2 > \left[1 + \langle \varpi_y^2 \rangle_i + \mu^2 \left(1 + \langle \varpi_y^2 \rangle_e\right)\right]/4, \tag{5}$$

where $\langle \varpi_y^2 \rangle_a = \int \mathrm{d}^2\varpi\, F_a \varpi_y^2$. Furthermore, the *total* length of the soliton wave, $|\Delta\zeta|$, and a typical timescale, Δt_0, in the comoving frame of the soliton are given through

$$|\Delta\zeta| \simeq z_{\mathrm{end}}(c/\omega_{p,i})(z_i A_{\max})^{1/2}\Gamma_b^{-3/2}(c/V_b)^{3/2}, \tag{6a}$$

$$\Delta t_0 = (\Gamma_b/c)(V_b/c)|\Delta\zeta| \simeq z_{\mathrm{end}}\omega_{p,i}^{-1}(z_i A_{\max})^{1/2}\Gamma_b^{-1/2}(c/V_b)^{1/2}, \tag{6b}$$

with $\omega_{p,i}^2 = 4\pi n e^2/M$ being the plasma frequency of the ions [17] and $\Gamma_b = \xi/(\xi^2-1)^{1/2}$ being the bulk Lorentz factor. The maxima of the magnetic and electric fields can then be described with

$$B_{\max}^2/8\pi = 2(1-R)^2 nMc^2(z_i A_{\max})(V_b/c)^3\Gamma_b^3, \tag{7a}$$

$$E_{\max}^2/8\pi = B_{\max}^2/(8\pi)(c/V_b)^2 = 2(1-R)^2 nMc^2(z_i A_{\max})(V_b/c)\Gamma_b^3. \tag{7b}$$

For comparison, note that in the interstellar medium where $B_{\mathrm{interstellar}} \simeq 3\ \mu\mathrm{G}$ and $n_{\mathrm{interstellar}} \simeq 0.1\ \mathrm{cm}^{-3}$, one has

$$B_{\mathrm{interstellar}}^2/(8\pi n_{\mathrm{interstellar}} Mc^2) \simeq 2\times 10^{-9}, \tag{8}$$

while in relativistic jets, for which $\Gamma_b \gtrsim 10^2$ and therefore $V_b \simeq c$, one has

$$B_{\max}^2/(8\pi nMc^2) \simeq 2\times 10^6(1-R)^2(z_i A_{\max})(\Gamma_b/100)^3 \tag{9}$$

representing field strengths of the order $90(1-R)(z_i A_{\max})^{1/2}(\Gamma_b/100)^{3/2}(n/0.1\ \mathrm{cm}^{-3})^{1/2}$ G where n is the number density in the jet, seen in the frame where the jet has a bulk speed V_b.

An overall upper bound for n_a can be found by considering the limitations due to (i) radiation, (ii) collision and (iii) degeneracy pressure of the electrons; these bounds also lead to an overall maximum magnetic field for the soliton. Each of the limitations gives slightly different limits, but they are all of the same order. In the case of radiation by electrons, one finds [17]

$$n_{\max} \leqslant \left[2.5\times 10^{33}/\langle 1+\varpi_y^2\rangle_e^2\right]\ \mathrm{cm}^{-3}, \tag{10a}$$

$$B_{\max} \leqslant 1.4\times 10^{19}(1-R)(z_i A_{\max})^{1/2}(\Gamma_b/100)^{3/2}/\langle 1+\varpi_y^2\rangle_e\ \mathrm{G}; \tag{10b}$$

for the collision of electrons, one has

$$n_{\max} \leqslant 2.2\times 10^{33}\frac{\Gamma_b(V_b/c)^3}{(z_i A_{\max})}\ \mathrm{cm}^{-3}, \tag{11a}$$

$$B_{\max} \leqslant 1.3\times 10^{20}(1-R)(\Gamma_b/100)\ \mathrm{G}, \tag{11b}$$

while the degeneracy pressure gives

$$n_{\max} \leqslant (mc/\hbar)^3 = 1.7\times 10^{31}\ \mathrm{cm}^{-3}, \tag{12a}$$

$$B_{\max} \leqslant 1.2\times 10^{18}(1-R)(z_i A_{\max})^{1/2}(\Gamma_b/100)^{3/2}\ \mathrm{G}. \tag{12b}$$

This short discussion provides the framework for the further calculation of radiation from the jets in GRBs, which will follow in the subsequent sections.

3. Development of the radiation field

The radiation field consists of the radiation of all the electrons interacting with the soliton as depicted in figure 2. Therefore, one first considers the radiation emission of a single electron accelerated by the wave. Then one can integrate over the electron distribution in the jet to obtain the total radiation field generated by the soliton.

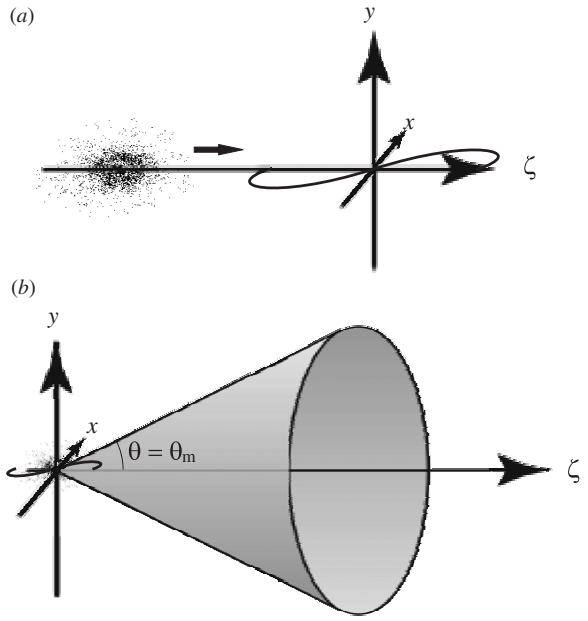

Figure 2. Geometry of the radiation in the rest frame of the soliton. (*a*) A bulk of electrons approaches the soliton. (*b*) When the electrons are deflected by the electric fields of the soliton, they emit radiation, mostly in a small cone along their direction of motion, which is typical for relativistic radiation. For the sake of clarity, the maximum angle θ_m of the cone is exaggerated.

3.1. The total power radiated

The radiated power of a single charged particle is, in general, defined by [18]

$$P = 2e^2/(3c)\gamma^6(\dot{\vec{\beta}}^2 - (\vec{\beta} \times \dot{\vec{\beta}})^2), \tag{13}$$

with $\vec{\beta} = \vec{v}/c$. As shown in [17] in the case of the soliton wave structure (with $W = eA/mc$), one obtains the radiated power from one electron as

$$P = 2e^2/(3c)\Gamma_b^2\left(1 + \varpi_y^2\right)(\dot{W}/c)^2. \tag{14}$$

The total radiated energy of one electron can be calculated [17] by integration over the nonlinear wave time or, by the substitution $\xi c\,\mathrm{d}t = \mathrm{d}\zeta = L\,\mathrm{d}z$, over the length of the soliton yielding (with $A = A_{\max}u$)

$$\mathcal{E} = \int P\,\mathrm{d}t = \frac{4e^2}{3\mu^2 L}(z_i A_{\max})^2 \frac{c}{V_b}\Gamma_b^2\left(1 + \varpi_y^2\right)\int_{R^2}^1 \mathrm{d}u \left|\frac{\partial u}{\partial z}\right|. \tag{15}$$

With the definition from equation (3),

$$I_R \equiv \int_{R^2}^1 \mathrm{d}u \left|\frac{\partial u}{\partial z}\right| = \int_{R^2}^1 \mathrm{d}u \frac{(1-u)^{1/2}(u-R^2)^{1/2}}{u^{1/2}}, \tag{16}$$

the radiated energy is given by

$$\mathcal{E} = (4e^2/3\mu^2 L)(z_i A_{\max})^2 (c/V_b)\Gamma_b^2\left(1 + \varpi_y^2\right) I_R. \tag{17}$$

3.2. Radiation emission of one electron

The differential intensity in the angular frequency range ω to $\omega + \mathrm{d}\omega$ and in the solid angle range Ω to $\Omega + \mathrm{d}\Omega$ is expressed [18] through

$$\frac{\mathrm{d}^2 I}{\mathrm{d}\omega\,\mathrm{d}\Omega} = \frac{e^2\omega^2}{4\pi^2 c}\left|\int_{-\infty}^{\infty}(\vec{n}\times(\vec{n}\times\vec{\beta}))\exp[\mathrm{i}\omega(t-\vec{n}\cdot\vec{r}(t)/c)]\,\mathrm{d}t\right|^2, \tag{18}$$

with the unit vector $\vec{n} = (n_x, n_y, n_z)$ (with $n_x^2 + n_y^2 + n_z^2 = 1$) in the line of sight. The particle velocity can be separated into a constant part and differences involving the varying potential A:

$$\beta_x \equiv \beta_{0,x} + \Delta\beta_x, \tag{19a}$$

$$\beta_y \equiv \beta_{0,y} + \Delta\beta_y, \tag{19b}$$

$$\beta_z = V_b/c = \xi^{-1}, \tag{19c}$$

with

$$\beta_{0,x} = \frac{\varpi_x - z_a R^2 A_{\max}}{\Gamma_b E_\perp[R^2 A_{\max}]}, \tag{20a}$$

$$\beta_{0,y} = \frac{\varpi_y}{\Gamma_b E_\perp[R^2 A_{\max}]}, \tag{20b}$$

the constant velocity components outside the soliton where $A = R^2 A_{\max}$ [17], and

$$\Delta\beta_x = \frac{1}{\Gamma_b}\left[\varpi_x\left(\frac{1}{E_\perp[A]} - \frac{1}{E_\perp[R^2 A_{\max}]}\right) - z_a\left(\frac{A}{E_\perp[A]} - \frac{R^2 A_{\max}}{E_\perp[R^2 A_{\max}]}\right)\right], \tag{21a}$$

$$\Delta\beta_y = \frac{\varpi_y}{\Gamma_b}\left(\frac{1}{E_\perp[A]} - \frac{1}{E_\perp[R^2 A_{\max}]}\right), \tag{21b}$$

the differences of the particle velocities within the soliton. Note that $\Delta\beta_x$ and $\Delta\beta_y$ are different from zero only in $|\zeta| = \left|Z_0 - \left(c^2 t/V_b\Gamma_b^2\right)\right| < \zeta_{\mathrm{end}}$. Then one obtains for the particle trajectory

$$X(t) = X_0 + \beta_{0,x} ct + c\int_{-\infty}^{t}\Delta\beta_x(t')\,\mathrm{d}t', \tag{22a}$$

$$Y(t) = Y_0 + \beta_{0,y} ct + c\int_{-\infty}^{t}\Delta\beta_y(t')\,\mathrm{d}t', \tag{22b}$$

$$Z(t) = Z_0 + V_b t. \tag{22c}$$

Note that large X, Y, Z has the dimension of length, while small x, y, z are dimensionless. The phase $\Phi(t) = \omega(t - \vec{n}\cdot\vec{r}(t)/c)$ in equation (18) can then be expressed in terms of the particle trajectories,

$$\Phi(t) \equiv \Phi_0 - \Delta\Phi, \tag{23}$$

with

$$\Phi_0 = \omega[t(1 - \vec{n}\cdot\vec{\beta}_0) - \vec{n}\cdot\vec{r}_0/c], \tag{24a}$$

$$\Delta\Phi = \omega\int_{-\infty}^{t}\mathrm{d}t'[n_x\Delta\beta_x(t') + n_y\Delta\beta_y(t')], \tag{24b}$$

where $\vec{r}_0 = (X_0, Y_0, Z_0)$ and $\vec{\beta}_0 = (\beta_{0,x}, \beta_{0,y}, V_b/c)$. Note that $\Delta\Phi(\zeta \leqslant -\zeta_{\rm end}) = 0$, but $\Delta\Phi(\zeta \geqslant \zeta_{\rm end}) = \Delta\Phi(\zeta_{\rm end}) \neq 0$. Thus, all the integrals in equation (18) are of the form

$$\int_{-\infty}^{\infty} {\rm d}t\, \vec{\beta}(t) \exp[{\rm i}\Phi(t)] \equiv \hat{J}, \tag{25}$$

leading to an alternative notation for equation (18):

$$\frac{{\rm d}^2 I}{{\rm d}\omega\, {\rm d}\Omega} = \frac{e^2\omega^2}{4\pi^2 c}|\vec{n} \times (\vec{n} \times \hat{J})|^2, \tag{26}$$

with

$$\hat{J}_\perp = \hat{J} - \vec{n}(\vec{n} \cdot \hat{J}). \tag{27}$$

The tedious evaluation of the integrals (25) is performed in appendix A in terms of two basic integrals:

$$\Delta\Phi(\zeta) = \omega\Lambda \int_{-\zeta_{\rm end}}^{\zeta} {\rm d}\zeta' [n_x \Delta\beta_x(\zeta') + n_y \Delta\beta_y(\zeta')], \tag{28a}$$

$$j_y = \int_{-\zeta_{\rm end}}^{\zeta_{\rm end}} {\rm d}\zeta \exp[{\rm i}\omega l\zeta - {\rm i}\Delta\Phi(\zeta)]\Delta\beta_y(\zeta), \tag{28b}$$

with $\Lambda = \left(V_b \Gamma_b^2 / c^2\right)$ and $l = (1 - \vec{n} \cdot \vec{\beta}_0)\Lambda$. These integrals allow one to write an expression leading to ${\rm d}^2 I/({\rm d}\omega\, {\rm d}\Omega)$ (as given in appendix A) because

$$\vec{j}_\perp \cdot \vec{j}_\perp{}^* = |\vec{j}_2|^2 - \frac{(\vec{n} - \vec{\beta}_0) \cdot [\vec{j}_2^*(\vec{n} \cdot \vec{j}_2) + \vec{j}_2(\vec{n} \cdot \vec{j}_2^*)]}{1 - (\vec{n} \cdot \vec{\beta}_0)} + \frac{|\vec{n} - \vec{\beta}_0|^2}{(1 - (\vec{n} \cdot \vec{\beta}_0))^2}|\vec{n} \cdot \vec{j}_2|^2, \tag{29}$$

where $\vec{j}_2 = (j_x, j_y, 0)$.

Now consider the particle motion of a single electron under the influence of the soliton wave. Within the range $-\zeta_{\rm end} \leqslant \zeta \leqslant \zeta_{\rm end}$, the electron motion is determined by the difference velocities $\Delta\beta_x, \Delta\beta_y$ as functions of ζ. Furthermore, there is a phase shift $\Delta\Phi(\zeta)$. The calculations of the velocities are given (to second order in ζ) in appendix B yielding

$$\begin{aligned} \Delta\vec{\beta} &\equiv \Delta\vec{\beta}_0(\zeta_{\rm end} - |\zeta|)^2 \qquad \text{in } \zeta_{\rm max} \leqslant |\zeta| \leqslant \zeta_{\rm end}, \quad \text{regime (a)}, \\ &\equiv \Delta\vec{\beta}_1 - \Delta\vec{\beta}_2\zeta^2 \qquad \text{in } 0 \leqslant |\zeta| \leqslant \zeta_{\rm max}, \quad \text{regime (b)}, \end{aligned} \tag{30}$$

where $\Delta\vec{\beta}_0$, $\Delta\vec{\beta}_1$ and $\Delta\vec{\beta}_2$ are given in appendix B. Regime (a) describes the outer region of the soliton, where the field strength drops to zero at $\zeta_{\rm end}$ from the maximum value at $\zeta_{\rm max}$, whereas regime (b) denotes the inner region in the interval $[-\zeta_{\rm max}, \zeta_{\rm max}]$. It was previously deduced [17] that a solitary wave exists only if both A and $A_{\rm max}$ are 'large', i.e. $|z_a A_{\rm max}| \gg \max\{1, |\varpi_x|, |\varpi_y|, |\varpi_z|\}$. This case describes particles in a strong field where the interaction time is long enough that the particles support the nonlinear wave. However, the soliton parameter R depends on $zA_{\rm max}$ itself, which will be represented in the following by

$$R = \left(\frac{G_2}{2G_0}\right)^{1/2} \frac{1}{A_{\rm max}} \equiv \frac{R'}{z_a A_{\rm max}}. \tag{31}$$

Note that R' is governed only by the distribution function F_a. Thus, $|z_a R^2 A_{\rm max}| = |(R')^2/(z_a A_{\rm max})| \ll \max\{1, |\varpi_x|, |\varpi_y|, |\varpi_z|\}$.

With the above definitions, from equations (30a) and (30b), one can calculate the integrals $\Delta\Phi$, j_x and j_y. Note that for $\Delta\Phi$, one intersects the wave in three regions:

$$\begin{aligned} \Delta\Phi_1(\zeta) &\equiv \Delta\Phi(-\zeta_{\rm end} \leqslant \zeta \leqslant -\zeta_{\rm max}) \\ &= \omega\Lambda(\vec{n} \cdot \Delta\vec{\beta}_0)(\zeta_{\rm end} + \zeta)^3/3, \end{aligned} \tag{32a}$$

$$\Delta\Phi_2(\zeta) \equiv \Delta\Phi(-\zeta_{\max} \leqslant \zeta \leqslant \zeta_{\max})$$
$$= \Delta\Phi_1(\zeta = -\zeta_{\max}) + \omega\Lambda\big[(\vec{n}\cdot\Delta\vec{\beta}_1)(\zeta_{\max}+\zeta) - (\vec{n}\cdot\Delta\vec{\beta}_2)\big(\zeta_{\max}^3+\zeta^3\big)/3\big], \quad (32b)$$

$$\Delta\Phi_3(\zeta) \equiv \Delta\Phi(\zeta_{\max} \leqslant \zeta \leqslant \zeta_{\text{end}})$$
$$= \Delta\Phi_2(\zeta = \zeta_{\max}) - \omega\Lambda(\vec{n}\cdot\Delta\vec{\beta}_0)[(\zeta_{\text{end}}-\zeta)^3 - (\zeta_{\text{end}}-\zeta_{\max})^3]/3. \quad (32c)$$

With this solution for $\Delta\Phi$, one can write the phase shift change of a particle after passing through the soliton as

$$\Delta\Phi(\zeta \geqslant \zeta_{\text{end}}) = \Delta\Phi(\zeta_{\text{end}}) = 2\omega\Lambda(\vec{n}\cdot\Delta\vec{\beta}_0)(\zeta_{\text{end}}-\zeta_{\max})^3/3$$
$$+2\omega\Lambda\zeta_{\max}\big[(\vec{n}\cdot\Delta\vec{\beta}_1) - (\vec{n}\cdot\Delta\vec{\beta}_2)\zeta_{\max}^2/3\big], \quad (33)$$

yielding (after the transformations $\zeta+\zeta_{\text{end}} \equiv \bar{\zeta}$ in solution (32*a*), $\zeta+\zeta_{\max} \equiv \bar{\zeta}$ in solution (32*b*) and $-\zeta+\zeta_{\text{end}} \equiv \bar{\zeta}$ in solution (32*c*), respectively)

$$j_y = \int_{-\zeta_{\text{end}}}^{-\zeta_{\max}} \Delta\beta_{0,y}(-\zeta_{\text{end}}-\zeta)^2 \exp[\mathrm{i}\omega l\zeta - \mathrm{i}\Delta\Phi_1(\zeta)]\,\mathrm{d}\zeta$$
$$+\int_{-\zeta_{\max}}^{\zeta_{\max}} (\Delta\beta_{1,y} - \Delta\beta_{2,y}\zeta^2)\exp[\mathrm{i}\omega l\zeta - \mathrm{i}\Delta\Phi_2(\zeta)]\,\mathrm{d}\zeta$$
$$+\int_{\zeta_{\max}}^{\zeta_{\text{end}}} \Delta\beta_{0,y}(\zeta_{\text{end}}-\zeta)^2\exp[\mathrm{i}\omega l\zeta - \mathrm{i}\Delta\Phi_3(\zeta)]\,\mathrm{d}\zeta$$
$$= \Delta\beta_{0,y}\bigg[\int_0^{\zeta_{\text{end}}-\zeta_{\max}} \mathrm{d}\bar{\zeta}\,\bar{\zeta}^2\exp[\mathrm{i}\omega l(\bar{\zeta}-\zeta_{\text{end}}) - \mathrm{i}\Delta\Phi_1(\bar{\zeta}-\zeta_{\text{end}})]$$
$$-\int_{\zeta_{\text{end}}-\zeta_{\max}}^{0} \mathrm{d}\bar{\zeta}\,\bar{\zeta}^2\exp[-\mathrm{i}\omega l(\bar{\zeta}-\zeta_{\text{end}}) - \mathrm{i}\Delta\Phi_3(-\bar{\zeta}+\zeta_{\text{end}})]\bigg]$$
$$+\int_0^{2\zeta_{\max}} \mathrm{d}\bar{\zeta}\,[\Delta\beta_{1,y} - \Delta\beta_{2,y}(\zeta_{\max}^2 - 2\zeta_{\max}\bar{\zeta}+\bar{\zeta}^2)]$$
$$\times\exp[\mathrm{i}\omega l(\bar{\zeta}-\zeta_{\max}) - \mathrm{i}\Delta\Phi_2(\bar{\zeta}-\zeta_{\max})]). \quad (34)$$

With the replacement of all explicit y subscripts by x subscripts in equation (34), one has the corresponding expression for j_x.

Note that in each integrand of j_x and j_y, one has the general exponential structure $\psi_0+\psi_1\bar{\zeta}+\psi_3\bar{\zeta}^3$. Thus, there is a basic integral type that can be written as

$$\int_0^{\mathcal{A}_j} \mathrm{d}\bar{\zeta}\,\bar{\zeta}^n\exp[\mathrm{i}\psi_{1,j}\bar{\zeta} + \mathrm{i}\psi_{3,j}\bar{\zeta}^3] \equiv M_n[\mathcal{A}_j;\psi_{1,j},\psi_{3,j}]. \quad (35)$$

First note that $\mathcal{A}_j \in \{\zeta_{\text{end}}-\zeta_{\max}, 2\zeta_{\max}\} > 0$. Second, note that $\psi_{1,j} \in \{\omega\Lambda(1-\vec{n}\cdot\vec{\beta}_0), \omega\Lambda(1-\vec{n}\cdot\vec{\beta}_0-\vec{n}\cdot\Delta\vec{\beta}_1)\} > 0$ because $\vec{n}\cdot\vec{\beta} \leqslant 1$. Thus, only $\psi_{3,j}$ can be either positive or negative and so one is interested in the two integrals

$$M_n^{\pm}[\mathcal{A}_j;\psi_{1,j},\psi_{3,j}] = \int_0^{\mathcal{A}_j} \mathrm{d}\bar{\zeta}\,\bar{\zeta}^n\exp[\mathrm{i}(\psi_{1,j}\bar{\zeta} \pm |\psi_{3,j}|\bar{\zeta}^3)]. \quad (36)$$

For later relevance, note that $\psi_{1,j}, |\psi_{3,j}| \propto \omega$.

For $\vec{j}_\perp$, one has to consider

$$j_y = \Delta\beta_{0,y}(M_2[\zeta_{\text{end}}-\zeta_{\max};\omega l, -\omega\Lambda(\vec{n}\cdot\Delta\vec{\beta}_0)/3]\exp[-\mathrm{i}\omega l\zeta_{\text{end}}]$$
$$+M_2[\zeta_{\text{end}}-\zeta_{\max};\omega l, -\omega\Lambda(\vec{n}\cdot\Delta\vec{\beta}_0)/3]^*\exp[\mathrm{i}\omega l\zeta_{\text{end}} - \mathrm{i}\Delta\Phi(\zeta_{\text{end}})])$$
$$+\big[\big(\Delta\beta_{1,y} - \Delta\beta_{2,y}\zeta_{\max}^2\big)M_0[2\zeta_{\max};\omega(l-\Lambda(\vec{n}\cdot\Delta\vec{\beta}_1)),\omega\Lambda(\vec{n}\cdot\Delta\vec{\beta}_2)/3]$$

$$+2\Delta\beta_{2,y}\zeta_{\max}M_1[2\zeta_{\max};\,\omega(l-\Lambda(\vec{n}\cdot\Delta\vec{\beta}_1)),\,\omega\Lambda(\vec{n}\cdot\Delta\vec{\beta}_2)/3]$$
$$-\Delta\beta_{2,y}M_2[2\zeta_{\max};\,\omega(l-\Lambda(\vec{n}\cdot\Delta\vec{\beta}_1)),\,\omega\Lambda(\vec{n}\cdot\Delta\vec{\beta}_2)/3]\big]$$
$$\times\exp[-\mathrm{i}\omega l\zeta_{\max}-\mathrm{i}\omega\Lambda(\vec{n}\cdot\Delta\vec{\beta}_0)(\zeta_{\mathrm{end}}-\zeta_{\max})^3/3]. \tag{37}$$

Then one can write down j_x (using the replacement of all explicit y subscripts by x subscripts) and subsequently $\vec{j}_\perp\cdot\vec{j}_\perp^{\,*}$ in terms of the integral $M_n[\mathcal{A}_j;\psi_{1,j},\psi_{3,j}]$. There remains then only the job of writing down the complete expression for the differential intensity spectrum once the M_n integrals are evaluated.

Note that one has to develop approximations for the integrals (36) as done in appendix C. Thus, one has two regimes with different approximations (30a) and (30b) and consequently six variables for the integral M_n, namely $\mathcal{A}_a$, $\psi_{1,a}$, $\psi_{3,a}$, $\mathcal{A}_b$, $\psi_{1,b}$ and $\psi_{3,a}$. In particular, the emerging scalar products $\vec{n}\cdot\Delta\vec{\beta}_0$ and $\vec{n}\cdot\Delta\vec{\beta}_2$ enable $\psi_{3,j}$ to change its sign yielding two different evaluations of M_n: case (1) for $\vec{n}\cdot\Delta\vec{\beta}_{0,2}>0$ and case (2) for $\vec{n}\cdot\Delta\vec{\beta}_{0,2}<0$.

It is useful to introduce characteristic lengths,

$$\zeta_{c,j}\equiv(\psi_{1,j}/3|\psi_{3,j}|)^{1/2}, \tag{38a}$$

and characteristic frequency ratios,

$$\omega/\omega_{c,j}\equiv\left(\psi_{1,j}^3/3|\psi_{3,j}|\right)^{1/2}, \tag{38b}$$

with $j\in\{a,b\}$. Note that all $\psi_{1,j}$ and $\psi_{3,j}$ are proportional to ω. Second, both the characteristic frequency and length are functions of the particle's momentum $\vec{\varpi}$ and the angle to the observer defined through $\vec{n}$.

There are three independent conditions for the differential frequency spectrum to be considered: the different regimes (a) and (b), the influence of the viewing angle leading to cases (1) and (2), and the low and high frequency ranges. Thus, eight different calculations have to be done. For the spectrum of one particle at a particular viewing angle, one has to consider both regimes of the soliton and then calculate the frequency approximations. Then if one is interested in the angular dependence of a distribution of particles, one has to include the angle effect.

3.3. The differential intensity spectrum for small and large frequencies

The approximations introduced above can be used to evaluate the spectrum for small and large frequencies. Two angular functions are of importance within the computations

$$S_1[\theta,\Gamma_b,\Phi]\equiv 1-\sqrt{1-\Gamma_b^{-2}}\cos\theta-(\sin\theta/\Gamma_b)\Phi, \tag{39}$$
$$S_2[\theta,\Gamma_b,\Psi]\equiv(\sin\theta/\Gamma_b)\Psi. \tag{40}$$

Details of these functions are given in appendix D.

At the end of each subsection, numerical calculations are given for an electron spectrum

$$F_a=\frac{\gamma-2}{2\pi}\frac{\delta(\varpi_z)}{\left(1+\varpi_x^2+\varpi_y^2+\varpi_z^2\right)^{\gamma/2}}. \tag{41}$$

We use dimensionless units with the normalizations $(\Lambda L)\omega$ and $(4\pi^2c/e^2)\,\mathrm{d}^2I/(\mathrm{d}\omega\,\mathrm{d}\Omega)$. For numerical estimations, parameter values used are

$$\begin{aligned}&\Gamma_b=10, && z_aA_{\max}=10\Rightarrow R=10^{-1} && (\text{for }\gamma=5),\\ &\varpi_{x,y}=10^{-2}, && \theta=\arcsin\Gamma_b^{-1}, && \phi=5\pi/4,\end{aligned} \tag{42}$$

unless otherwise prescribed.

For low frequencies, one has the differential intensity spectrum (appendix E):

$$\frac{\mathrm{d}^2 I}{\mathrm{d}\omega\,\mathrm{d}\Omega} \simeq \frac{e^2}{4\pi^2 c}\left(\frac{\omega}{\omega_0}\right)^2. \tag{43}$$

This result is limited by the condition

$$\omega \ll \omega_{\mathrm{low}} \equiv (\Lambda \mathcal{A}_j S_1)^{-1}. \tag{44}$$

Thus for low frequencies, one has dipole radiation.

In the high frequency regime (see appendix F) there arise different approximations, depending on the scalar products $\vec{n}\cdot\vec{\Delta\beta}_{0,2}$. For $|\vec{n}\cdot\vec{\Delta\beta}_{0,2}| \gg 0$ one obtains two different solutions, depending on whether the scalar products $(\vec{n}\cdot\vec{\Delta\beta}_{0,2})$ are positive or negative, yielding different results with respect to the angle between the velocity perturbations and the line of sight. The first solution (except for $1/(2\Gamma_b) \leqslant \theta \leqslant 2/\Gamma_b$) is given by

$$\frac{\mathrm{d}^2 I}{\mathrm{d}\omega\,\mathrm{d}\Omega} \simeq \frac{e^2}{4\pi^2 c}\frac{\pi\omega}{\omega_{c,b}\sin^2\theta\sin^2\phi}\exp\left[-\frac{4\omega}{3\omega_{c,b}}\right]. \tag{45}$$

The second solution (where $1/(2\Gamma_b) \leqslant \theta \leqslant 2/\Gamma_b$) is obtained similarly, yielding

$$\frac{\mathrm{d}^2 I}{\mathrm{d}\omega\,\mathrm{d}\Omega} \simeq \frac{e^2}{4\pi^2 c}\frac{2\pi\Gamma_b^2\omega}{\omega_{c,a}\cos^2\phi}. \tag{46}$$

The parameters $\omega_{c,a}$ and $\omega_{c,b}$ are defined in appendix F. Both solutions are limited by

$$\omega \gg \omega_{\mathrm{high}} \equiv \begin{cases} 3\big/\big(\Lambda\mathcal{A}_b^3 S_{2,b}\big), & \theta \notin [1/(2\Gamma_b),\, 2/\Gamma_b] \\ (\Lambda\mathcal{A}_a S_{1,a})^{-1}, & \theta \in [1/(2\Gamma_b),\, 2/\Gamma_b]. \end{cases} \tag{47}$$

If $\vec{n}\cdot\vec{\Delta\beta}_{0,2} \simeq 0$ (within an interval $[(2k+1)\pi/2 - \Delta\phi_a/2,\,(2k+1)\pi/2 + \Delta\phi_a/2]$ in regime (a) and $[k\pi - \Delta\phi_b/2,\, k\pi + \Delta\phi_b/2]$ in regime (b), where $\Delta\phi_{a,b}(\Gamma_b, z_a A_{\max}, \theta, \omega)$ is given in appendix F.4 and $k = 0, 1$), then one has

$$\frac{\mathrm{d}^2 I}{\mathrm{d}\omega\,\mathrm{d}\Omega} \simeq \frac{e^2\alpha^2}{4\pi^2 c} = \mathrm{const}, \tag{48}$$

with α being given in appendix F and a lower limit for the frequency

$$\omega \gg \omega^*_{\mathrm{high}} \equiv (\Lambda\mathcal{A}_a S_{1,a})^{-1}. \tag{49}$$

Note that there exists a high frequency problem. If integrated over $\omega_{\mathrm{high}} \leqslant \omega \leqslant \infty$, equation (46) (and similarly equation (48)) would yield an infinite amount of radiation. However, one knows [17] that the emitted energy of one electron is exactly limited to

$$\mathcal{E} = \frac{e^2}{4\pi^2 c}\frac{16\pi^2}{3\mu^2}(\Lambda L)^{-1}\Gamma_b^4 I_R\big(1+\varpi_y^2\big)(z_i A_{\max})^2, \tag{50}$$

with I_R being given in equation (16) and $\mu = m_e/m_i$. Thus, there is an 'edge' in the differential frequency spectrum at high frequencies where the electron has lost all its energy. This restriction allows one to find the maximum $\omega_{\max}$ to which the radiation can exist by writing

$$\begin{aligned}\mathcal{E} &= \int \mathrm{d}\Omega \int_0^{\omega_{\max}} \mathrm{d}\omega \frac{\mathrm{d}^2 I}{\mathrm{d}\omega\,\mathrm{d}\Omega} \\ &\simeq \frac{e^2}{4\pi^2 c}\left[\int_A \mathrm{d}\Omega \int_0^{\omega_*} \frac{\omega^2}{\omega_0^2} + 2\pi\Gamma_b^2 \int_A \mathrm{d}\Omega \int_{\omega_*}^{\omega_{\max}} \mathrm{d}\omega \frac{\omega}{\cos^2\phi\,\omega_{c,a}}\right. \\ &\quad \left. + \int_B \mathrm{d}\Omega \int_0^{\omega_{*,\alpha}} \frac{\omega^2}{\omega_0^2} + \int_B \mathrm{d}\Omega \int_{\omega_{*,\alpha}}^{\omega_{\max}} \alpha^2\right]\end{aligned}$$

$$= \frac{e^2}{4\pi^2 c}\left[\frac{4\pi^3\Gamma_b^6}{3}\int_A \mathrm{d}\Omega \frac{\omega_0^4}{\cos^6\phi\,\omega_{c,a}^3} - \frac{2}{3}\int_B \mathrm{d}\Omega\,\alpha^3\omega_0 \right.$$
$$\left. + \omega_{\max}\int_B \mathrm{d}\Omega\,\alpha^2 + \omega_{\max}^2 2\pi\Gamma_b^2\int_A \mathrm{d}\Omega\frac{1}{\cos^2\phi\,\omega_{c,a}}\right]. \tag{51}$$

Here, A and B denote the regimes where $\vec{n}\cdot\vec{\Delta\beta}_{0,2} \gg 0$ and $\vec{n}\cdot\vec{\Delta\beta}_{0,2} \simeq 0$, respectively. Equation (51) can be rearranged to yield the quadratic equation for $\omega_{\max}$:

$$0 = \omega_{\max}^2\left[\pi\Gamma_b^2\int_A \mathrm{d}\Omega\frac{1}{\cos^2\phi\,\omega_{c,a}}\right] + \omega_{\max}\left[\int_B \mathrm{d}\Omega\,\alpha^2\right]$$
$$-\left[\frac{4\pi^2 c\mathcal{E}}{e^2} - \frac{4\pi^3\Gamma_b^6}{3}\int_A \mathrm{d}\Omega\frac{\omega_0^4}{\cos^6\phi\,\omega_{c,a}^3} + \frac{2}{3}\int_B \mathrm{d}\Omega\,\alpha^3\omega_0\right], \tag{52}$$

where $\mathcal{E}$, ω_*, ω_0 and $\omega_{c,a}$ are functions of $\vec{n}$ and $\vec{\varpi}$.

3.4. Intermediate values

There exist intermediate values, ω_*, between the two regimes of low and high frequencies depending on the high frequency approximation. For $|\vec{n}\cdot\vec{\Delta\beta}_{0,2}| \gg 0$, ω_* is characterized by the equation

$$\omega_* = \left(2\pi\Gamma_b^2/\cos^2\phi\right)\left(\omega_0^2/\omega_{c,a}\right), \tag{53}$$

for regime (a), and for regime (b) by

$$\omega_* = (3/4)\omega_{c,b}W\left[(4\pi/(3\sin^2\theta\sin^2\phi))\left(\omega_0^2/\omega_{c,b}^2\right)\right], \tag{54}$$

where $W[x]$ denotes the Lambert W function, i.e. the solution $y \equiv W[x]$ of the equation $x = y\exp[y]$.

For the high frequency solution (48), one has an intermediate value

$$\omega_{*,\alpha} = \alpha\omega_0. \tag{55}$$

Characteristic curves of the differential frequency spectrum are shown in figure 3 for various polar angles $\theta = 10^{-6}, 0.1, 0.3$. Note that approximation (48) applies for small θ; for $\theta \simeq 1/\Gamma_b$, the spectrum is given by equation (46); for larger polar angles, approximation (45) is valid. Thus, most of the energy is radiated within a cone of angle $\theta_m = \arcsin\Gamma_b^{-1} \simeq \Gamma_b^{-1}$, as shown in figure 4 for a frequency of $\omega = 10^4/(\Lambda L)$ and $\phi = 3\pi/2$, typical for relativistic particles. Therefore, the main contribution of the radiation (at least for the given example) is directly connected with the outer region (a) of the soliton. This result is not surprising, because the numbers chosen yield $R = 0.1$ which has—as can be estimated from figure 1—a relative large gradient of the magnetic field between $z_{\max}$ and z_{end} leading to strong radiation. Note that both large gradients $\mathrm{d}b/\mathrm{d}x$ (at the beginning and at the end of the soliton) are positive.

3.5. Integration over a distribution of particles

For the electron power-law distribution (41),

$$F_a = \frac{\gamma - 2}{2\pi}\frac{\delta(\varpi_z)}{\left(1 + \varpi_x^2 + \varpi_y^2 + \varpi_z^2\right)^{\gamma/2}}, \tag{56}$$

with $\gamma \geqslant 4$, one now calculates the radiation spectrum. The frequency limits ω_{low} and ω_{high} are functions of the momenta $p_j \in \{\varpi_x, \varpi_y, \varpi_z\}$. However, because the real spectrum must have a smooth transition between the two regimes, such can be approximated by using both regimes

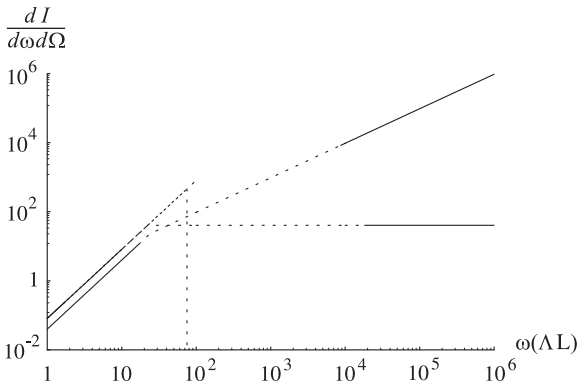

Figure 3. Characteristic curve shapes for the radiation in terms of $\omega(\Lambda L)$ of the electrons for various polar angles θ, with $\theta_a = 10^{-6}, \theta_b = 0.1$ and $\theta_c = 0.3$. The dashed lines are the continuation of the graphs for the regions where the low frequency and high frequency approximations are not accurate.

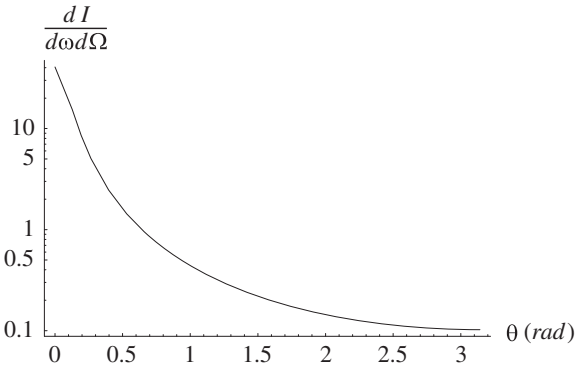

Figure 4. The differential intensity as a function of θ for a frequency of $\omega = 10^4/(\Lambda L)$ and $\phi = 3\pi/2$.

to first order in ω_*. Formulae (43), (45) and (46) have been derived for $|p_j| \ll |z_a A_{\max}|$. However, because the distribution function tends to zero as $\varpi \to \infty$, the high-ϖ part to the integral is negligible. Consequently, one has to compute the integral

$$\int \mathrm{d}\varpi^3 F_a \frac{\mathrm{d}^2 I}{\mathrm{d}\omega\, \mathrm{d}\Omega} = \frac{e^2}{4\pi^2 c} \frac{2(\gamma-2)}{\pi} \int_0^\infty \mathrm{d}\varpi_x \int_0^\infty \mathrm{d}\varpi_y \frac{1}{\left(1+\varpi_x^2+\varpi_y^2\right)^{\gamma/2}} \times \left(\frac{\omega^2}{\omega_0^2} H[\omega_*(\varpi_x, \varpi_y) - \omega] + \frac{2\pi \Gamma_b^2 \omega}{\cos^2 \phi \omega_{c,a}} H[\omega - \omega_*(\varpi_x, \varpi_y)] \right). \quad (57)$$

Because $|\omega_*(\varpi_x, \varpi_y) - \omega|$ cannot be rearranged to obtain analytic constraints for ϖ_x or ϖ_y, the solution of the integral (57) can be performed numerically only. For the polar angle where most radiation is beamed, $\theta_m = 0.1$, the result is illustrated in figure 5. Note that this curve is of comparable magnitude and slopes as its counterpart in figure 3.

3.6. Viewing angle effect

Here we consider the behavior of the viewing angle for one electron. First, the polar variation gives the relativistic beaming into the propagation direction as shown in figure 4. For the

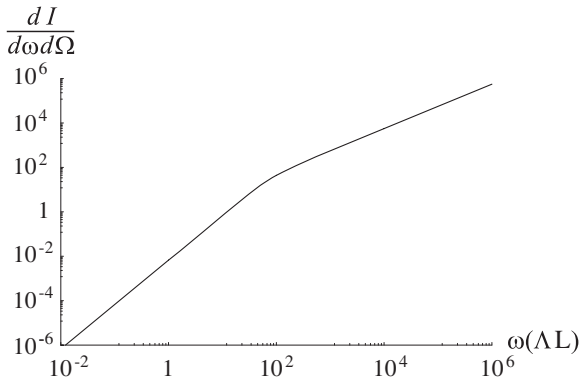

Figure 5. Radiation of an ensemble of electrons for a polar angle $\theta = 0.1$.

azimuth angle, one has to consider the parameters ω_0 (for the maximum at $\theta_m \simeq \Gamma_b^{-1}$) and $\omega_{c,j}$ from equations (43), (45) and (46). Apart from sine or cosine terms, each has a factor containing trigonometric functions of ϕ and ϖ_j (with $B_j = \varpi_j \big/ \left(1 + \varpi_x^2 + \varpi_y^2\right)^{1/2}$):

$$\omega_0 \propto |(\sin\phi - B_y)(1 + B_x) - (\cos\phi - B_x)B_y|, \tag{58a}$$

$$\omega_{c,a} \propto \left|\sin\phi\varpi_x\varpi_y - \cos\phi\left(1 + \varpi_y^2\right)\right|^{1/2}, \tag{58b}$$

$$\omega_{c,b} \propto |\sin\phi\varpi_y|^{1/2}. \tag{58c}$$

Such factors can be zero for particular azimuths yielding apparent poles in the spectrum. However, such poles are prevented because the approximation (48) is valid, which has no pole. Thus, for very small momenta for equations (43) and (45) one has the estimation $\phi \simeq 0, \pi$ describing a plane *parallel* to the soliton direction of motion, comparable to synchrotron radiation, but solution (46) is remarkably different. Here the azimuth angles are $\phi \simeq \pi/2$, $3\pi/2$, exhibiting the main radiation contribution *perpendicular* to the plane of motion.

Now one is interested in the azimuthal distribution of the total radiation from one electron. Therefore, it is necessary to first perform the ω-integral in equations (43) and (46), because these contribute most to the spectrum. Carrying out the integrations, one obtains

$$\frac{\mathrm{d}I}{\mathrm{d}\Omega} = \frac{e^2}{4\pi^2 c}\left(\frac{\pi\Gamma_b^2}{\cos^2\phi}\frac{\omega_{\max}^2}{\omega_{c,a}} - \frac{4\pi^3\Gamma_b^6}{3\cos^6\phi}\frac{\omega_0^4}{\omega_{c,a}^3}\right), \tag{59}$$

where $\omega_{\max}$ is the maximum frequency from equation (52).

The parameters that have an angular dependence on equation (59) are ω_0 (for $\theta_m \simeq \Gamma_b^{-1}$) and $\omega_{c,a}$ as given in appendices appendix D and appendix F. Numerical results are shown in figure 6 for a maximum frequency $\omega_{\max} = 10^6/(\Lambda L)$. First, note that both terms have maxima at $\phi \simeq \pi/2, 3\pi/2$ unlike synchrotron radiation. However, the existence of poles in equation (59) is prevented analogous to equations (43), (45) and (46). Second, note that for a high $\omega_{\max}$ the first term in equation (59) dominates and the azimuthal variation can be well described by $|\cos\phi|^{-5/2}$.

4. Polarization and Faraday effect

In this section, we consider the polarization and Faraday rotation of the soliton radiation. For later comparison note that synchrotron radiation is polarized mostly parallel to the plane of the electron trajectory [18].

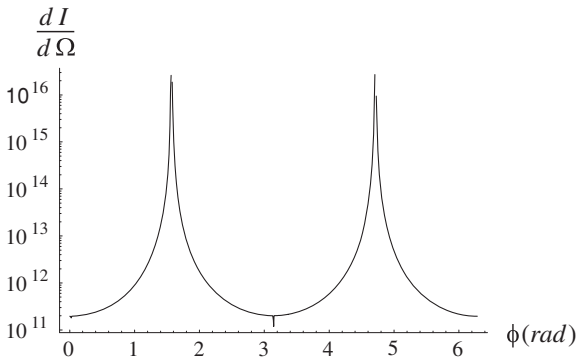

Figure 6. The frequency-integrated differential intensity as a function of ϕ for a given $\omega_{\max} = 10^6/(\Lambda L)$ and the parameters given in equation (42).

4.1. Polarization

For polarization, one has to specify two perpendicular unit vectors and the line of sight direction given by $\vec{n}$. For the radiation process, choose the direction of the electric field of the soliton as a reference, that is, the unit vector $\vec{e}_x = (1, 0, 0)$. The polarization vectors are then given by

$$\begin{aligned} \vec{e}_\parallel &= \frac{\vec{e}_x - (\vec{n}\cdot\vec{e}_x)\vec{n}}{\varepsilon} = \frac{1}{\varepsilon}\begin{pmatrix} \cos^2\theta + \sin^2\theta\sin^2\phi \\ -\sin^2\theta\cos\phi\sin\phi \\ -\cos\theta\sin\theta\cos\phi \end{pmatrix}, \\ \vec{e}_\perp &= \vec{n}\times\vec{e}_\parallel = \frac{1}{\varepsilon}\begin{pmatrix} 0 \\ \cos\theta \\ -\sin\theta\sin\phi \end{pmatrix}, \end{aligned} \tag{60}$$

where

$$\varepsilon = (\cos^2\theta + \sin^2\theta\sin^2\phi)^{1/2} \tag{61}$$

normalizes both polarization vectors. For the polar angle $\theta_m = \arcsin\Gamma_b^{-1}$ (where an electron radiates most), the polarization vectors are approximately

$$\vec{e}_\parallel \simeq (1, 0, -\cos\phi/\Gamma_b), \qquad \vec{e}_\perp \simeq (0, 1, -\sin\phi/\Gamma_b) \tag{62}$$

for $\Gamma_b \gg 1$.

The differential intensity spectrum for each polarization vector is given in general by [18]

$$\left(\frac{\mathrm{d}^2 I}{\mathrm{d}\omega\,\mathrm{d}\Omega}\right)_{\parallel,\perp} = \frac{e^2\omega^2}{4\pi^2 c}|\vec{e}_{\parallel,\perp}\cdot[\vec{n}\times(\vec{n}\times\hat{J})]|^2, \tag{63}$$

yielding

$$\begin{aligned} \left(\frac{\mathrm{d}^2 I}{\mathrm{d}\omega\,\mathrm{d}\Omega}\right)_\parallel &= \frac{e^2\omega^2}{4\pi^2 c}\frac{\Lambda^2}{\varepsilon^2}\left|j_x - \frac{\sin\theta\cos\phi - \beta_{0,x}}{1-\vec{n}\cdot\vec{\beta}_0}(\vec{n}\cdot\vec{j}_2)\right|^2, \\ \left(\frac{\mathrm{d}^2 I}{\mathrm{d}\omega\,\mathrm{d}\Omega}\right)_\perp &= \frac{e^2\omega^2}{4\pi^2 c}\frac{\Lambda^2}{\varepsilon^2}\left|\cos\theta j_y - \frac{\sin\theta\sin\phi\left(1-\Gamma_b^{-2}\right)^{1/2} - \cos\theta\beta_{0,y}}{1-\vec{n}\cdot\vec{\beta}_0}(\vec{n}\cdot\vec{j}_2)\right|^2. \end{aligned} \tag{64}$$

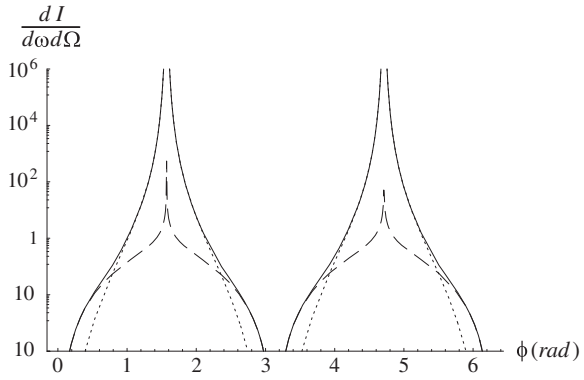

Figure 7. The differential intensity divided into the fractions polarized parallel (dotted) and perpendicular (dashed) to the plane of the soliton as a function of ϕ for $\omega = 10^1/(\Lambda L)$ and the parameters given in equation (42). The solid line labels the combined differential intensity. The parallel polarization dominates the radiation.

For $\theta = 0$, the spectra simplify to

$$\left(\frac{\mathrm{d}^2 I}{\mathrm{d}\omega\,\mathrm{d}\Omega}\right)_{\parallel} = \frac{e^2\omega^2}{4\pi^2 c}\Lambda^2|j_x|^2, \qquad \left(\frac{\mathrm{d}^2 I}{\mathrm{d}\omega\,\mathrm{d}\Omega}\right)_{\perp} = \frac{e^2\omega^2}{4\pi^2 c}\Lambda^2|j_y|^2. \tag{65}$$

For $\theta = \theta_m$ and $\Gamma_b \gg 1$, one finds

$$\left(\frac{\mathrm{d}^2 I}{\mathrm{d}\omega\,\mathrm{d}\Omega}\right)_{\parallel} \simeq \frac{e^2\omega^2}{4\pi^2 c}\Lambda^2 \sin^2\phi \left|\frac{(\sin\phi - B_y)j_x - (\cos\phi - B_x)j_y}{1 - (\cos\phi B_x + \sin\phi B_y)}\right|^2, \tag{66a}$$

$$\left(\frac{\mathrm{d}^2 I}{\mathrm{d}\omega\,\mathrm{d}\Omega}\right)_{\perp} \simeq \frac{e^2\omega^2}{4\pi^2 c}\Lambda^2 \cos^2\phi \left|\frac{(\sin\phi - B_y)j_x - (\cos\phi - B_x)j_y}{1 - (\cos\phi B_x + \sin\phi B_y)}\right|^2. \tag{66b}$$

Note the similarity of solutions (66*a*) and (66*b*), and equation (A.24), apart from the sine and cosine terms. Thus, the polarization of the maximum radiation depends dominantly on the azimuthal angle to the line of sight and the soliton propagation direction for θ_m. If the observer is above or below the plane of the soliton by an angle θ_m, one has radiation polarized parallel to the plane; otherwise, in the soliton plane, the observer sees a perpendicular polarized beam. However, as depicted in figure 7, the emission is concentrated at angles $\phi \simeq \pi/2, 3\pi/2$, so that the radiation is, in general, polarized parallel to the electric field of the soliton. Such is shown in figure 8.

4.2. Faraday effect

The Faraday effect describes the rotation of the polarization plane due to the magnetic fields of the medium through which the radiation propagates:

$$\delta\alpha = \frac{2\pi e^3}{m_e^2 c^2}\frac{1}{\omega^2}\int_A^B n_e \vec{B}\cdot \mathrm{d}\vec{l}, \tag{67}$$

where z is the straight path of one photon with frequency ω from a point between the location of emission and the soliton, A, to a point B between the soliton to the observer. First, consider that the photon passes the soliton at a displacement $\hat{\zeta} = L\hat{z}$ between both ends of the soliton, $-\zeta_{\mathrm{end}} \leqslant \hat{\zeta} \leqslant \zeta_{\mathrm{end}}$. (The displacement variables $\hat{z}, \hat{\zeta}$ are hatted to distinguish them from

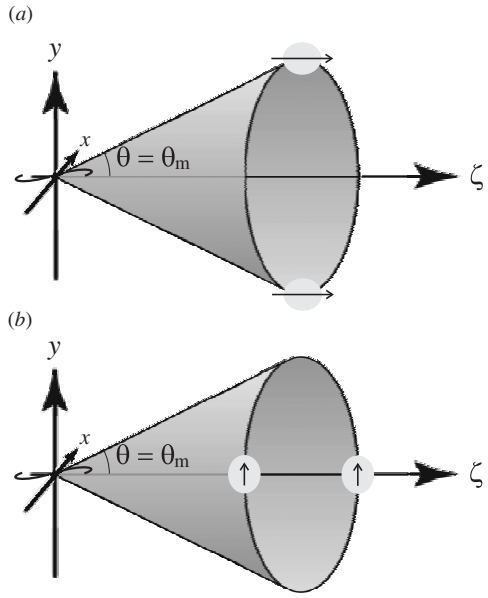

Figure 8. Polarization of the emitted radiation for $\theta \simeq \theta_m$ as a function of the azimuthal angle ϕ. The soliton is represented by its electric fields in the x-direction. (a) For azimuthal angles $\phi = \pi/2, 3\pi/2$, one has parallel polarization. (b) Azimuthal angles $\phi = 0, \pi$ yield perpendicular polarization. However, the intensity is considerably less than in the parallel case (cf figure 7).

spacial variables z, ζ.) Second, consider that the soliton has a finite size perpendicular to the z-direction, modeled here by Gaussian structures. Then the magnetic field can be written as (with $x = X/W$, $y = Y/W$ and $z = \zeta/L$)

$$\vec{B}(X, Y, \zeta) = (1 - R)^2 \frac{A_{\max}}{L} b(\zeta/L) \exp\left(-\frac{X^2 + Y^2}{\kappa^2 L^2}\right) \vec{e}_y, \tag{68}$$

where $\kappa = W/L$ gives, approximately, the ratio of width W and length scales L. The curvature (to B from A) has the parametric representation

$$C = L \begin{pmatrix} t \sin\theta \cos\phi \\ t \sin\theta \sin\phi \\ t \cos\theta + \hat{z} \end{pmatrix}, \tag{69}$$

with $t \in [t_A, t_B]$. Because the photon is considered to pass through the whole soliton, one can extend both limits to $\pm\infty$.

If the density is constant, one has

$$\delta\alpha = \frac{\omega_{p,e}^2}{2\omega^2}(1 - R)^2 z_e \frac{A_{\max}}{L} \sin\theta \sin\phi L \int_{-\infty}^{\infty} \mathrm{d}t \exp\left(-\frac{\sin^2\theta}{\kappa^2} t^2\right) b(\hat{z} + t\cos\theta), \tag{70}$$

where $\omega_{p,e}^2 = 4\pi n_e e^2/m_e$, the local plasma frequency, and $z_e = e/(m_e c^2)$.

Equation (70) can be calculated performing a Fourier transformation of $b(\hat{z} + t\cos\theta)$, yielding

$$\begin{aligned}\delta\alpha &\simeq \frac{\kappa}{2^{3/2}} \frac{\omega_{p,e}^2}{\omega^2}(1 - R)^2 z_e A_{\max} \sin\phi \int_{-\infty}^{\infty} \mathrm{d}k\, b(k)\, \mathrm{e}^{\mathrm{i}\hat{z}k} \exp[-\kappa^2 \cot^2\theta k^2/4] \\ &\simeq \kappa \frac{\pi^{1/2}}{2} \frac{\omega_{p,e}^2}{\omega^2}(1 - R)^2 z_e A_{\max} \sin\phi b(\hat{z}),\end{aligned} \tag{71}$$

where the last approximation is valid for polar angles $\theta \gg \arctan(\kappa/2)$.

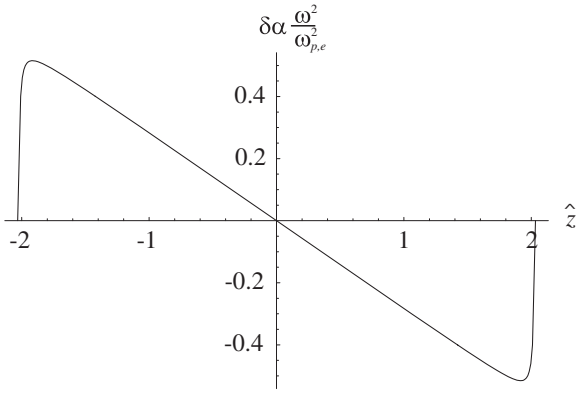

Figure 9. The Faraday rotation $\delta\alpha(\omega^2/\omega_{p,e}^2)$ for a photon traversing at a soliton with a dimensionless displacement $\hat{z} = \hat{\zeta}/L$. The numerical result is computed with the parameters given in equation (42).

Numerical results for the Faraday rotation $\delta\alpha\left(\omega^2/\omega_{p,e}^2\right)$ described by equation (71) as a function of the displacement $\hat{z}$ are given in figure 9. Note that the Faraday rotation is closely related to the magnetic field shown in figure 1. In the case of small angles θ, the integration over θ averages the contribution of the magnetic field creating a curve with lower gradients and a lower maximum. For $\theta = 0$, equivalent to traversing the whole soliton, the Faraday effect vanishes.

5. Discussion and conclusion

Previously [17], we presented the theory of self-consistent solitons that can produce radiation in relativistic plasmas without an explicit background magnetic field. We considered this radiation effect for the case of the origin of GRBs. The favored fireball scenario yields, in interaction with ambient matter, shock waves that can accelerate charged particles—most prominently, electrons and protons [23].

The question of the energy output of the particles is mostly referred to as synchrotron radiation and inverse Compton scattering. However, the first process of energy dissipation requires the presence of a background magnetic field. Until now, the origin and the mechanism for such a field have been discussed intensely [24–26]. Other radiation processes should be taken into account.

As we have shown, nonlinear solitary waves can arise from a relativistic, but nonmagnetized, plasma. The main variable that has to be considered is the differential frequency spectrum of a single electron. Then, one is able to investigate the influence of the viewing angle to both calculate the spectrum for a total ensemble of particles and to examine the polarization. In principle, the method of obtaining the differential frequency spectrum is similar to that for synchrotron radiation. The basic difference is that for synchrotron radiation the magnetic field is considered to be constant and the electron moves in circles perpendicular to the magnetic field, while in the case of the soliton the electrons move mostly linearly and are deflected via the Lorentz force. Thus, the radiation is not produced by acceleration through a constant background field but, instead, is caused by an interaction of the electrons with highly varying magnetic and electric fields.

For illustration purposes, we chose numerical values for the parameters: $\Gamma_b = 10$, $z_a A_{\max} = 10$, $\varpi_{x,y} = 10^{-2}$, $\theta = \arcsin \Gamma_b^{-1}$ and $\phi = 5\pi/4$, unless mentioned otherwise. The results of the numerical calculations are such that most of the radiation stems from the outer regions of the soliton near the final points, described with equation (46), and is radiated into a cone with the polar angle $\theta \simeq \Gamma_b^{-1}$. This outcome is coincident with the well-known fact that the radiation of relativistic particles is generally concentrated in this rather small solid angle.

However, there arise significant differences relative to synchrotron radiation: the azimuthal variation is different. For one particle, the viewing angle effect results in radiation orientated mostly *perpendicular* to the electron trajectory. This orientation persists even for a whole ensemble of electrons. The polarization depends on the azimuthal angle of the line of sight and the electron trajectory given by the soliton plane with perpendicular polarization at particular angles and unveils a major difference to synchrotron radiation by having a parallel polarization as well.

The Faraday effect allows the observer to measure extraterrestrial magnetic fields, e.g., in other galaxies. For the soliton, the Faraday effect has a dependence that is related closely to the form of the magnetic field of the soliton.

Overall, we have presented a fundamental treatment of the radiation produced by the interaction of electrons with solitary waves that can arise in the unmagnetized plasma of an astrophysical relativistic jet. The value of this model is that one can bypass the question of the origin of the magnetic fields, which are a fundamental prerequisite needed for synchrotron radiation. More detailed numerical computations could avoid the separation of at least three solutions for the differential intensity spectrum given in equation (43), (45) and (46). Likewise, more detailed numerical simulations of the soliton–electron interaction may emphasize more the differences between synchrotron and soliton radiation.

Acknowledgments

This work was partially supported by the Deutsche Forschungsgemeinschaft through grant no. Schl 201/19-1, through the Sonderforschungsbereich 591, and through the award of a Mercator Professorship to one of the authors (IL).

Appendix A. Evaluation of the integrals $\hat{J}$

A.1. General reduction

In equation (25),

$$\hat{J} = \int_{-\infty}^{\infty} \mathrm{d}t\, \vec{\beta}(t) \exp[\mathrm{i}\Phi(t)] \equiv \Lambda \vec{J}, \tag{A.1}$$

with $\Lambda = \left(V_b \Gamma_b^2 / c^2\right)$, one first performs a substitution to the coordinate ζ via

$$\zeta = (t/\Lambda) - Z_0 \qquad \text{in} \quad -\zeta_{\mathrm{end}} \leqslant \zeta \leqslant \zeta_{\mathrm{end}}. \tag{A.2}$$

Thus, $t = (\zeta + Z_0)\Lambda$.

Then one can transform the integral ignoring the constant phase $\varphi_0 = \exp[-\mathrm{i}\omega(\vec{n} \cdot \vec{r}_0/c)]$ and with $l = (1 - \vec{n} \cdot \vec{\beta}_0)\Lambda$ (note that $\vec{\Delta\beta} = 0$ for $|\zeta| > \zeta_{\mathrm{end}}$) to obtain

$$\begin{aligned} \vec{J}/\varphi_0 &= \int_{-\infty}^{\infty} \mathrm{d}\zeta\, \vec{\beta}(\zeta) \exp[\mathrm{i}\Phi(\zeta)]/\varphi_0 \\ &= \int_{-\zeta_{\mathrm{end}}}^{\zeta_{\mathrm{end}}} \mathrm{d}\zeta (\vec{\beta}_0 + \vec{\Delta\beta}(\zeta)) \exp[\mathrm{i}\omega l\zeta - \mathrm{i}\Delta\Phi(\zeta)] \end{aligned}$$

$$+\vec{\beta}_0\left(\int_{-\infty}^{-\zeta_{\rm end}} {\rm d}\zeta\,\exp[{\rm i}\omega l\zeta - {\rm i}\Delta\Phi(\zeta)] + \int_{\zeta_{\rm end}}^{\infty} {\rm d}\zeta\,\exp[{\rm i}\omega l\zeta - {\rm i}\Delta\Phi(\zeta)]\right) \equiv \vec{j}. \quad \text{(A.3)}$$

With $\Delta\Phi(\zeta \leqslant -\zeta_{\rm end}) = 0$ and $\Delta\Phi(\zeta \geqslant \zeta_{\rm end}) = \Delta\Phi(\zeta_{\rm end}) \neq 0$ for the last two integrals in equation (A.3), one has

$$\begin{aligned}\int_{-\infty}^{-\zeta_{\rm end}} {\rm d}\zeta\,\exp[{\rm i}\omega l\zeta - {\rm i}\Delta\Phi(\zeta)] + \int_{\zeta_{\rm end}}^{\infty} {\rm d}\zeta\,\exp[{\rm i}\omega l\zeta - {\rm i}\Delta\Phi(\zeta)] \\ = \exp[-{\rm i}\omega l\zeta_{\rm end}]/({\rm i}\omega l) - \exp[-{\rm i}\Delta\Phi(\zeta_{\rm end})]\exp[{\rm i}\omega l\zeta_{\rm end}]/({\rm i}\omega l) \\ = -(2/\omega l)\exp[-{\rm i}\Delta\Phi(\zeta_{\rm end})/2]\sin[\omega l\zeta_{\rm end} - \Delta\Phi(\zeta_{\rm end})/2] \equiv -S. \quad \text{(A.4)}\end{aligned}$$

With the same substitution $t' = (\zeta' + Z_0)\Lambda$ in

$$\begin{aligned}\Delta\Phi &= \omega\int_{-\infty}^{t} {\rm d}t'[n_x\Delta\beta_x(t') + n_y\Delta\beta_y(t')] \\ &= \omega\Lambda\int_{-\zeta_{\rm end}}^{\zeta} {\rm d}\zeta'[n_x\Delta\beta_x(\zeta') + n_y\Delta\beta_y(\zeta')], \quad \text{(A.5)}\end{aligned}$$

one obtains

$$\vec{j} \equiv \vec{j}_1 + \vec{j}_2, \quad \text{(A.6)}$$

with one term involving the constant velocity $\vec{\beta}_0$ and one term involving the difference vector $\vec{\Delta\beta}$, so that

$$\vec{j}_1 = \vec{\beta}_0\int_{-\zeta_{\rm end}}^{\zeta_{\rm end}} {\rm d}\zeta\,\exp[{\rm i}\omega l\zeta - {\rm i}\Delta\Phi(\zeta)] - \vec{\beta}_0 S, \quad \text{(A.7)}$$

$$\vec{j}_2 = \int_{-\zeta_{\rm end}}^{\zeta_{\rm end}} {\rm d}\zeta\,\exp[{\rm i}\omega l\zeta - {\rm i}\omega\Delta\Phi(\zeta)](\Delta\beta_x(\zeta), \Delta\beta_y(\zeta), 0) \equiv (j_x, j_y, 0). \quad \text{(A.8)}$$

A.2. Considerations on $|\vec{n}\cdot\vec{j}|^2$ and $\vec{j}_\perp\cdot\vec{j}_\perp{}^*$

For equation (26), one has to evaluate $\vec{j}_\perp\cdot\vec{j}_\perp{}^*$. Consider $\vec{n}\cdot\vec{j} = j_\parallel$,

$$j_\parallel \equiv (\vec{n}\cdot\vec{\beta}_0)(I_1 - S) + I_2, \quad \text{(A.9)}$$

with the two integrals

$$I_1 = \int_{-\zeta_{\rm end}}^{\zeta_{\rm end}} {\rm d}\zeta\,\exp[{\rm i}\omega l\zeta - {\rm i}\Delta\Phi(\zeta)], \quad \text{(A.10)}$$

$$\begin{aligned}I_2 = (\vec{n}\cdot\vec{j}_2) = \int_{-\zeta_{\rm end}}^{\zeta_{\rm end}} {\rm d}\zeta\,\exp[{\rm i}\omega l\zeta](n_x\Delta\beta_x(\zeta) + n_y\Delta\beta_y(\zeta)) \\ \times\exp\left[-{\rm i}\omega\Lambda\int_{-\zeta_{\rm end}}^{\zeta} {\rm d}\zeta'(n_x\Delta\beta_x(\zeta') + n_y\Delta\beta_y(\zeta'))\right]. \quad \text{(A.11)}\end{aligned}$$

The second term, I_2, can be expressed in terms of I_1 by partial integration:

$$\begin{aligned}I_2 = n_x j_x + n_y j_y &= -\frac{\rm i}{\omega\Lambda}\int_{-\zeta_{\rm end}}^{\zeta_{\rm end}} {\rm d}\zeta\,\exp[{\rm i}\omega l\zeta]\frac{\rm d}{{\rm d}\zeta}\exp[-{\rm i}\Delta\Phi(\zeta)] \\ &= -(2/\omega\Lambda)\exp[-{\rm i}\Delta\Phi(\zeta_{\rm end})/2]\sin[\omega l\zeta_{\rm end} - \Delta\Phi(\zeta_{\rm end})/2] + (l/\Lambda)I_1 \\ &= (l/\Lambda)(I_1 - S). \quad \text{(A.12)}\end{aligned}$$

Using equations (A.9) and (A.12) for the parallel parts of the integrals in equation (26), one can write

$$j_{\parallel} = I_1 - S = (\Lambda/l)(\vec{n}\cdot\vec{j}_2), \tag{A.13}$$

because $(\vec{n}\cdot\vec{\beta}_0) + (l/\Lambda) = 1$.

With Equations (A.7) and (A.13) for $\vec{j}_1$, one then obtains

$$\vec{j}_1 = \vec{\beta}_0(I_1 - S) = (\Lambda/l)\vec{\beta}_0(\vec{n}\cdot\vec{j}_2). \tag{A.14}$$

Thus, one has to solve only the integrals $\Delta\Phi(\zeta_{\rm end})$, j_x and j_y to obtain $\vec{j}_\perp$. Note that j_x and j_y are symmetric, so the evaluation of j_y automatically yields the solution for j_x by replacing the y subscripts by x subscripts.

Then, with $\vec{j} = (\Lambda/l)\vec{\beta}_0(\vec{n}\cdot\vec{j}_2) + \vec{j}_2$ and $(\Lambda/l) = (1 - (\vec{n}\cdot\vec{\beta}_0))^{-1}$, one can write

$$\vec{j}_\perp = \vec{j} - \vec{n}(\vec{n}\cdot\vec{j}) = \vec{j}_2 - \frac{\vec{n}-\vec{\beta}_0}{1-(\vec{n}\cdot\vec{\beta}_0)}(\vec{n}\cdot\vec{j}_2), \tag{A.15}$$

yielding

$$\begin{aligned}\vec{j}_\perp\cdot\vec{j}_\perp{}^* &= \left|\vec{j}_2 - \frac{\vec{n}-\vec{\beta}_0}{1-(\vec{n}\cdot\vec{\beta}_0)}(\vec{n}\cdot\vec{j}_2)\right|^2 \\ &= |\vec{j}_2|^2 - \frac{(\vec{n}-\vec{\beta}_0)\cdot[\vec{j}_2^*(\vec{n}\cdot\vec{j}_2) + \vec{j}_2(\vec{n}\cdot\vec{j}_2^*)]}{1-(\vec{n}\cdot\vec{\beta}_0)} + \frac{|\vec{n}-\vec{\beta}_0|^2}{(1-(\vec{n}\cdot\vec{\beta}_0))^2}|\vec{n}\cdot\vec{j}_2|^2. \end{aligned}\tag{A.16}$$

A.3. Behavior of $|\vec{j}_\perp|^2$

With the definitions

$$B_x = \Gamma_b\beta_{0,x} = \frac{\varpi_x - z_a R^2 A_{\max}}{E_\perp[R^2 A_{\max}]} < 1 \qquad B_y = \Gamma_b\beta_{0,y} = \frac{\varpi_y}{E_\perp[R^2 A_{\max}]} < 1 \tag{A.17}$$

and the vectors $\vec{n} = (\sin\theta\cos\phi, \sin\theta\sin\phi, \cos\theta)$, $\vec{\beta}_0 = (B_x/\Gamma_b, B_y/\Gamma_b, \left(1-\Gamma_b^{-2}\right)^{1/2})$ and $\vec{j} = (j_x, j_y, 0)$, one has for equation (A.16):

$$\begin{aligned}|\vec{j}_\perp|^2 = \Big[&\Big(\cos\theta - \sqrt{1-\Gamma_b^{-2}}\Big)^2|\cos\phi j_x + \sin\phi j_y|^2 \\ &+ \Big|\Big(\Big(1-\sqrt{1-\Gamma_b^{-2}}\cos\theta\Big)\sin\phi - \sin\theta B_y/\Gamma_b\Big)j_x \\ &- \Big(\Big(1-\sqrt{1-\Gamma_b^{-2}}\cos\theta\Big)\cos\phi - \sin\theta B_x/\Gamma_b\Big)j_y\Big|^2\Big] \\ &\times\Big(1-\sqrt{1-\Gamma_b^{-2}}\cos\theta - \sin\theta(\cos\phi B_x + \sin\phi B_y)/\Gamma_b\Big)^{-2}. \end{aligned}\tag{A.18}$$

Series expansion for large Γ_b yields

$$|\vec{j}_\perp|^2 = |j_x|^2 + |j_y|^2 + \frac{\sin\theta}{(1-\cos\theta)\Gamma_b}|(\cos\phi j_x + \sin\phi j_y)(B_x j_x + B_y j_y)| + \mathcal{O}\big(\Gamma_b^{-2}\big). \tag{A.19}$$

This expansion is valid as long as $\sin\theta/[(1-\cos\theta)\Gamma_b] \ll 1$, which for small angles is

$$\theta \gg 2/\Gamma_b. \tag{A.20}$$

Otherwise, for small angles one can approximate $\sin\theta \simeq \theta$, $\cos\theta \simeq 1$ leading to

$$|\vec{j}_\perp|^2 = |j_x|^2 + |j_y|^2 + \frac{\theta}{\Gamma_b(1-\left(1-\Gamma_b^{-2}\right)^{1/2}}|(\cos\phi j_x + \sin\phi j_y)(B_x j_x + B_y j_y)| + \mathcal{O}(\theta^2). \tag{A.21}$$

This result has a constraint given by $\theta/\left[\Gamma_b(1-\left(1-\Gamma_b^{-2}\right)^{1/2}\right] \ll 1$, which can be simplified for large Γ_b to

$$\theta \gg 1/(2\Gamma_b). \tag{A.22}$$

Thus, one has

$$|\vec{j}_\perp|^2 \simeq |j_x|^2 + |j_y|^2 \tag{A.23}$$

except for the interval $\theta \in [1/(2\Gamma_b), 2/\Gamma_b]$, where one can approximate $\theta \simeq \arcsin[1/\Gamma_b] + \epsilon$ leading to

$$|\vec{j}_\perp|^2 = \frac{(\sin\phi - B_y)^2|j_x|^2 + (\cos\phi - B_x)^2|j_y|^2 - (\cos\phi - B_x)(\sin\phi - B_y)(j_x j_y^* + j_x^* j_y)}{[1-(\cos\phi B_x + \sin\phi B_y)]^2} + \mathcal{O}(\epsilon^2). \tag{A.24}$$

Therefore, equation (A.24) may reach values substantially larger than equations (A.19) and (A.21).

Appendix B. The motion of the electrons

Write $u = A/A_{\max}$ as the normalized vector potential. Then u satisfies the equation (see in [17])

$$(\mathrm{d}u/\mathrm{d}z)^2 = (1-u)(u-R^2)/u, \tag{B.1}$$

where $(\mathrm{d}u/\mathrm{d}z)$ has a peak value on $u = R$. Furthermore, one has $u(z=0) = 1$ and $u(z = z_{\mathrm{end}}) = R^2$. The solution to equation (B.1) cannot be written in a closed analytical form; thus, one needs good approximations for $u(z)$. Because $u(z)$ is symmetric in z, in $1 \geqslant u \geqslant R$ choose

$$u = 1 - bz^2 \tag{B.2}$$

to obtain from equation (B.1), to order z^2,

$$b = (1-R^2)/4. \tag{B.3}$$

Then from the peak value (occurring on $u = R$), one finds the locations $z_{\max}$ as

$$z(u=R) = \pm\frac{2}{(1+R)^{1/2}} \equiv \pm z_{\max}, \tag{B.4}$$

with $z_{\max} > 0$. Similarly, one can write in $R \geqslant u \geqslant R^2$

$$u = R^2(1 + a(z_{\mathrm{end}} - |z|)^2), \tag{B.5}$$

which, when used in equation (B.1), yields

$$a = (1-R^2)/(4R^4), \tag{B.6}$$

to order z^2. Because $u(z = z_{\max}) = R$ and $u = R^2$ on $|z| = z_{\mathrm{end}}$, one finds the locations z_{end} as

$$z(u=R^2) = \pm[z_{\max} + 2R^{3/2}(1+R)^{-1/2}] = \pm 2\frac{1+R^{3/2}}{(1+R)^{1/2}} \equiv \pm z_{\mathrm{end}}, \tag{B.7}$$

with $z_{\mathrm{end}} > z_{\max} > 0$. Hence, one has two regimes:

$$\begin{aligned} u(z) &= 1 - (1-R^2)z^2/4 \equiv 1 - bz^2 \\ &\quad \text{in } 0 \leqslant |z| \leqslant z_{\max}, \\ u(z) &= R^2 + (1-R^2)(z_{\mathrm{end}} - |z|)^2/4R^2 \equiv R^2 + R^2 a(z_{\mathrm{end}} - |z|)^2 \\ &\quad \text{in } z_{\max} \leqslant |z| \leqslant z_{\mathrm{end}}. \end{aligned} \tag{B.8}$$

Now consider $\vec{\Delta\beta}$ from equations (19*a*) and (19*b*) with

$$E_\perp[A] = \left(1 + \varpi_y^2 + (\varpi_x - z_a A)^2\right)^{1/2}. \tag{B.9}$$

Because $u = A/A_{\max}$ is calculated to the *quadratic* order in z in the two regimes, $\Delta\beta_x$ and $\Delta\beta_y$ are also calculated to the quadratic order. The development is straightforward, albeit tedious. In $z_{\max} \leqslant |z| \leqslant z_{\text{end}}$, one has for the differences in equations (21*a*) and (21*b*)

$$\frac{1}{E_\perp[A]} - \frac{1}{E_\perp[R^2 A_{\max}]} = \frac{z_a R^2 A_{\max}(\varpi_x - z_a R^2 A_{\max})}{E_\perp^3[R^2 A_{\max}]} a(z_{\text{end}} - |z|)^2, \tag{B.10}$$

$$\frac{A}{E_\perp[A]} - \frac{R^2 A_{\max}}{E_\perp[R^2 A_{\max}]} = \left(1 + \frac{z_a R^2 A_{\max}(\varpi_x - z_a R^2 A_{\max})}{E_\perp^2[R^2 A_{\max}]}\right) \frac{R^2 A_{\max}}{E_\perp[R^2 A_{\max}]} a(z_{\text{end}} - |z|)^2; \tag{B.11}$$

thus, $\Delta\beta_x$, $\Delta\beta_y$ are known to order $z^2 = \zeta^2/L^2$. In $0 \leqslant |z| \leqslant z_{\max}$, one has the differences

$$\frac{1}{E_\perp[A]} - \frac{1}{E_\perp[R^2 A_{\max}]} = \frac{1}{E_\perp[A_{\max}]} - \frac{1}{E_\perp[R^2 A_{\max}]} - \frac{z_a A_{\max}(\varpi_x - z_a A_{\max})}{E_\perp^3[A_{\max}]} b z^2, \tag{B.12}$$

$$\frac{A}{E_\perp[A]} - \frac{R^2 A_{\max}}{E_\perp[R^2 A_{\max}]} = \frac{A_{\max}}{E_\perp[A_{\max}]} - \frac{R^2 A_{\max}}{E_\perp[R^2 A_{\max}]} - \left(1 + \frac{z_a A_{\max}(\varpi_x - z_a A_{\max})}{E_\perp^2[A_{\max}]}\right) \frac{A_{\max}}{E_\perp[A_{\max}]} b z^2. \tag{B.13}$$

Thus, $\Delta\beta_x$ and $\Delta\beta_y$ are also known to order $z^2 = \zeta^2/L^2$. In summary, one has

$$\begin{aligned} \vec{\Delta\beta} &\equiv \vec{\Delta\beta}_0(\zeta_{\text{end}} - |\zeta|)^2 \qquad \text{in} \quad \zeta_{\max} \leqslant |\zeta| \leqslant \zeta_{\text{end}}, \\ &\equiv \vec{\Delta\beta}_1 - \vec{\Delta\beta}_2 \zeta^2 \qquad \text{in} \quad 0 \leqslant |\zeta| \leqslant \zeta_{\max}, \end{aligned} \tag{B.14}$$

with the factors

$$\Delta\beta_{0,x} = -\frac{1 - R^2}{4L^2 R^2} \frac{z_a A_{\max}\left(1 + \varpi_y^2\right)}{\Gamma_b E_\perp^3[R^2 A_{\max}]}, \tag{B.15}$$

$$\Delta\beta_{0,y} = \frac{1 - R^2}{4L^2 R^2} \frac{z_a A_{\max} \varpi_y (\varpi_x - z_a R^2 A_{\max})}{\Gamma_b E_\perp^3[R^2 A_{\max}]}, \tag{B.16}$$

$$\Delta\beta_{1,x} = \frac{1}{\Gamma_b} \left(\frac{\varpi_x - z_a A_{\max}}{E_\perp[A_{\max}]} - \frac{\varpi_x - z_a R^2 A_{\max}}{E_\perp[R^2 A_{\max}]} \right), \tag{B.17}$$

$$\Delta\beta_{1,y} = \frac{\varpi_y}{\Gamma_b} \left(\frac{1}{E_\perp[A_{\max}]} - \frac{1}{E_\perp[R^2 A_{\max}]} \right), \tag{B.18}$$

$$\Delta\beta_{2,x} = -\frac{1 - R^2}{4L^2} \frac{z_a A_{\max}\left(1 + \varpi_y^2\right)}{\Gamma_b E_\perp^3[A_{\max}]}, \tag{B.19}$$

$$\Delta\beta_{2,y} = \frac{1 - R^2}{4L^2} \frac{z_a A_{\max} \varpi_y (\varpi_x - z_a A_{\max})}{\Gamma_b E_\perp^3[A_{\max}]}. \tag{B.20}$$

Note that $|\Delta\beta_{0,x}| \geqslant |\Delta\beta_{2,x}|$ and $|\Delta\beta_{0,y}| \geqslant |\Delta\beta_{2,y}|$ because $R \leqslant 1$. For later purposes, one needs to develop the factors for the case $|z_a A_{\max}| \gg \max\{1, |\varpi_j|\}$ with $j \in \{x, y, z\}$, but

note that $|z_a R^2 A_{\max}| = |(R')^2/(z_a A_{\max})| \ll \max\{1, |\varpi_j|\}$. First, consider the perpendicular energy. One obtains

$$E_\perp[A_{\max}]^{-m} = \left[1 + \varpi_y^2 + (\varpi_x - z_a A_{\max})^2\right]^{-m/2} \simeq \frac{1}{|z_a A_{\max}|^m}\left[1 + \frac{m\varpi_x}{z_a A_{\max}} + \frac{m\left[(m+1)\varpi_x^2 - \left(1+\varpi_y^2\right)\right]}{2(z_a A_{\max})^2}\right] \tag{B.21}$$

and

$$E_\perp[R^2 A_{\max}]^{-m} \simeq \frac{1}{E_0^m}\left[1 + \frac{m\varpi_x R'}{z_a A_{\max} E_0} + \frac{m\left[(m+1)\varpi_x^2 - \left(1+\varpi_y^2\right)\right](R')^2}{2(z_a A_{\max})^2 E_0^2}\right], \tag{B.22}$$

with $E_0^2 = 1 + \varpi_x^2 + \varpi_y^2$.

Thus one has approximations for the components (20*a*), (20*b*) and (B.15)–(B.20) which can be used later (assuming that $z_a A_{\max} > 0$):

$$B_x \simeq \frac{\varpi_x}{E_0}, \tag{B.23}$$

$$B_y \simeq \frac{\varpi_y}{E_0}, \tag{B.24}$$

$$\Delta\beta_{0,x} \simeq -\frac{1}{4L^2(R')^2\Gamma_b}(z_a A_{\max})^3 \frac{1+\varpi_y^2}{E_0^3}, \tag{B.25}$$

$$\Delta\beta_{0,y} \simeq \frac{1}{4L^2(R')^2\Gamma_b}(z_a A_{\max})^3 \frac{\varpi_x\varpi_y}{E_0^3}, \tag{B.26}$$

$$\Delta\beta_{1,x} \simeq -\frac{1}{\Gamma_b}\left(1 + \frac{\varpi_x}{E_0}\right) = -\frac{1+B_x}{\Gamma_b}, \tag{B.27}$$

$$\Delta\beta_{1,y} \simeq -\frac{1}{\Gamma_b}\frac{\varpi_y}{E_0} = -\frac{B_y}{\Gamma_b}, \tag{B.28}$$

$$\Delta\beta_{2,x} \simeq -\frac{1}{4L^2\Gamma_b}\frac{1}{(z_a A_{\max})^2}\left(1+\varpi_y^2\right), \tag{B.29}$$

$$\Delta\beta_{2,y} \simeq -\frac{1}{4L^2\Gamma_b}\frac{1}{z_a A_{\max}}\varpi_y. \tag{B.30}$$

Note for later relevance the various powers of $z_a A_{\max}$ of these components.

Appendix C. Approximations for the integral $M_n^{\pm}[\mathcal{A}_j; \psi_{1,j}, \psi_{3,j}]$

For clarity, in this section the index j is omitted for the variables $\mathcal{A}_j$, $\psi_{1,j}$ and $\psi_{3,j}$, because the results do not depend on the regimes of the soliton in detail. Because one is interested in the ranges with low frequency ($\omega \to 0$) and high frequency ($\omega \to \infty$), and $\psi_1, |\psi_3| \propto \omega$, one has to consider the cases $\psi_1, |\psi_3| \to 0$ and $\psi_1, |\psi_3| \to \infty$. Note that $|\psi_3| \to 0$ even for high ω for a vanishing scalar product $|\vec{n} \cdot \vec{\Delta\beta}_{0,2}|$. Thus, one has to investigate three cases.

C.1. $\psi_1, |\psi_3| \to 0$

Beginning with the definition of $M_n^{\pm}[\mathcal{A}; \psi_1, \psi_3]$ with $\bar{\zeta} = \mathcal{A}w$ and $\mathcal{A} = \text{const}$, one obtains

$$\int_0^{\mathcal{A}} \mathrm{d}\bar{\zeta}\, \bar{\zeta}^n \exp[\mathrm{i}(\psi_1\bar{\zeta} \pm |\psi_3|\bar{\zeta}^3)] = \mathcal{A}^{n+1}\int_0^1 \mathrm{d}w\, w^n \exp[\mathrm{i}\mathcal{A}(\psi_1 w \pm \mathcal{A}^2|\psi_3|w^3)]$$

$$\simeq \mathcal{A}^{n+1} \int_0^1 \mathrm{d}w\, w^n = \mathcal{A}^{n+1}/(n+1). \tag{C.1}$$

Note that this approximation is valid only for $\psi_1 \mathcal{A} \ll 1$ and $|\psi_3|\mathcal{A}^3 \ll 1$ leading (with definitions (38*a*) and (38*b*)) to conditions for the frequency given by

$$\omega \ll \omega_{\mathrm{low}} \equiv \min[(\zeta_c/\mathcal{A})\omega_c, 3(\zeta_c/\mathcal{A})^3\omega_c]. \tag{C.2}$$

C.2. $\psi_1, |\psi_3| \to \infty$

Here, one has $\psi_1 \mathcal{A} \gg 1$ and $|\psi_3|\mathcal{A}^3 \gg 1$ for $|\vec{n} \cdot \vec{\Delta}\beta_{0,2}| \gg 0$. Thus a lower limit to the frequency is, in analogy to the previous subsection, given by

$$\omega \gg \omega_{\mathrm{high}} \equiv \max[(\zeta_c/\mathcal{A})\omega_c, 3(\zeta_c/\mathcal{A})^3\omega_c]. \tag{C.3}$$

Perform the substitution $\bar{\zeta} = (\psi_1/|\psi_3|)^{1/2} w$, yielding

$$\begin{aligned}(\psi_1/|\psi_3|)^{-(n+1)/2} M_n^{\pm}[\mathcal{A}; \psi_1, \psi_3] &= \int_0^B \mathrm{d}w\, w^n \exp[\mathrm{i}k(w \pm w^3)] \\ &= \int_0^B \mathrm{d}w \exp[\Phi(w)] \equiv N_n^{\pm}[B; k],\end{aligned} \tag{C.4}$$

where $k \equiv \left(\psi_1^3/|\psi_3|\right)^{1/2} \propto \omega$, $B \equiv \mathcal{A}(\psi_1/|\psi_3|)^{-1/2}$, and

$$\Phi(w) = \mathrm{i}k(w \pm w^3) + n \ln[w]. \tag{C.5}$$

Because $k \propto \omega$, the integrand oscillates rapidly for almost all values of w except around the stationary phase points w_{sp} where the first derivation of $\Phi(w)$ has a zero. Hence it is justified to approximate the integral through a Taylor expansion around the points w_{sp}, which are given through $\Phi'(w_{\mathrm{sp}}) = \mathrm{i}k\left(1 \pm 3w_{\mathrm{sp}}^2\right) + (n/w_{\mathrm{sp}}) = 0$. One can approximate each of the cases in turn.

C.2.1. $1 + 3w_{\mathrm{sp}}^2 = (\mathrm{i}n/kw_{\mathrm{sp}})$. Because the integrand has no singularity, one can evaluate the integral $N_n^+[B; k]$ in the complex plane by a contour integral containing w_{sp}. Because $k \gg 1$, one has the solution (to second order) $w_{\mathrm{sp}}^{\pm} \simeq \pm\mathrm{i}/3^{1/2} - (\mathrm{i}n/2k)$ yielding $\Phi\left(w_{\mathrm{sp}}^{\pm}\right) \simeq \mp 2k/3^{3/2} + n \ln\left[w_{\mathrm{sp}}^{\pm}\right]$. One has to choose the upper signed root, because the lower sign leads to an integrand > 1. After Taylor expansion around w_{sp}^+, leading to

$$\Phi(w) \simeq \Phi\left(w_{\mathrm{sp}}^+\right) - (2 \cdot 3^{1/2}k - 3n)\left(w - w_{\mathrm{sp}}^+\right)^2/2 \tag{C.6}$$

and, further, with integration from $-\infty$ to ∞, one has

$$\begin{aligned}N_n^+[B; k] &\simeq (2\pi/(2 \cdot 3^{1/2}k - 3n))^{1/2}(i/3^{1/2})^n \exp[-2k/3^{3/2}] \\ &\simeq (\pi/3^{1/2}k)^{1/2}(i/3^{1/2})^n \exp[-2k/3^{3/2}].\end{aligned} \tag{C.7}$$

C.2.2. $1 - 3w_{\mathrm{sp}}^2 = (\mathrm{i}n/kw_{\mathrm{sp}})$. Here, the individual steps are almost the same. Because $k \gg 1$, the values of w_{sp} are located almost on the real axis and therefore dominate the value of the integral N_n^-. Hence, it is of importance to determine whether $\Re[w_{\mathrm{sp}}]$ lies between the integral endpoints. One has to choose the root with $\Re[w_{\mathrm{sp}}] > 0$. There is the constraint $\Re[w_{\mathrm{sp}}] \leqslant B$ (i.e. the phase point lies in the integral range) yielding

$$\mathcal{A}^2(\psi_1/|\psi_3|)^{-1} \geqslant 1/3 \quad \leftrightarrow \quad \mathcal{A}^2 \geqslant \zeta_c^2. \tag{C.8}$$

Note that for each particle ζ_c depends on the particle velocity and, furthermore, on the line of sight to the observer, so one cannot exclude any possibility. If constraint (C.8) is *not* fulfilled,

the integral N_n^- is small in comparison with the case where the constraint *is* fulfilled. Hence, one can neglect N_n^- for those particles with $\mathcal{A} < \zeta_c$. When inequality (C.8) is satisfied one has the stationary phase point $w_{\rm sp} \simeq 1/3^{1/2} - (in/2k)$, yielding

$$\Phi(w) \simeq \Phi(w_{\rm sp}) - (2 \cdot 3^{1/2} ik + 3n)(w - w_{\rm sp})^2/2 \tag{C.9}$$

and

$$\begin{aligned} N_n^-[B; k] &\simeq (2\pi/(2 \cdot 3^{1/2} \mathrm{i}k + 3n))^{1/2} (1/3^{1/2})^n \exp[2\mathrm{i}k/3^{3/2}] \\ &\simeq (\pi/3^{1/2}k)^{1/2} \, \mathrm{e}^{-\mathrm{i}\pi/4} (1/3^{1/2})^n \exp[2\mathrm{i}k/3^{3/2}]. \end{aligned} \tag{C.10}$$

C.3. $\psi_1 \to \infty, |\psi_3| \to 0$

Even for high ω it is possible that $|\psi_3| \to 0$, namely in the neighborhood of the angles where $S_2 \equiv |\vec{n} \cdot \vec{\Delta\beta}_{0,2}| \simeq 0$. For very high ω, it may be that there is only a very small range where one has $\psi_1 \to \infty$ and $|\psi_3| \to 0$, but that range has to be considered. The function S_2 is examined in detail in the following appendix. One has

$$\begin{aligned} \int_0^{\mathcal{A}} \mathrm{d}\bar{\zeta} \, \bar{\zeta}^n \exp[\mathrm{i}(\psi_1 \bar{\zeta} \pm |\psi_3| \bar{\zeta}^3)] &= \int_0^{\mathcal{A}} \mathrm{d}\bar{\zeta} \, \bar{\zeta}^n \exp[\mathrm{i}\psi_1 \bar{\zeta}(1 \pm (|\psi_3|/\psi_1)\bar{\zeta}^2)] \\ &\simeq \int_0^{\mathcal{A}} \mathrm{d}\bar{\zeta} \, \bar{\zeta}^n \exp[\mathrm{i}\psi_1 \bar{\zeta}] = \frac{\partial^n}{i^n \partial \psi_1^n} \int_0^{\mathcal{A}} \mathrm{d}\bar{\zeta} \exp[\mathrm{i}\psi_1 \bar{\zeta}] \\ &= \frac{\partial^n}{i^n \partial \psi_1^n} (\exp[\mathrm{i}\psi_1 \mathcal{A}] - 1)/(\mathrm{i}\psi_1) \\ &\simeq (\mathcal{A}^n/\mathrm{i}\psi_1) \exp[\mathrm{i}\psi_1 \mathcal{A}] - \delta_{n0}/(\mathrm{i}\psi_1), \end{aligned} \tag{C.11}$$

where in the last step $\psi_1 \to \infty$ and δ_{n0} is the Kronecker delta. Now one has to estimate the limits of this approximation. One has the constraints $\psi_1 \mathcal{A} \gg 1$ and $|\psi_3| \mathcal{A}^3 \ll 1$. The first condition gives

$$\begin{aligned} \omega \gg \omega^*_{\rm high} \equiv (\zeta_c/\mathcal{A})\omega_c &= 1/(\Lambda \mathcal{A}(1 - \vec{n} \cdot \vec{\beta}_0)), \quad \text{regime (a)} \\ &= 1/(\Lambda \mathcal{A}(1 - \vec{n} \cdot \vec{\beta}_0 - \vec{n} \cdot \vec{\Delta\beta}_1)), \quad \text{regime (b)}, \end{aligned} \tag{C.12}$$

whereas the second condition yields

$$\omega \ll 3(\zeta_c/\mathcal{A})^3 \omega_c = 1/(\Lambda \mathcal{A}^3 |\vec{n} \cdot \vec{\Delta\beta}_{0,2}|) \to \infty, \tag{C.13}$$

with $|\vec{n} \cdot \vec{\Delta\beta}_{0,2}| \to 0$. Thus, constraint (C.13) is not a constraint in the neighborhood of $|\vec{n} \cdot \vec{\Delta\beta}_{0,2}| = 0$ where equation (C.11) is valid.

Appendix D. The properties of the angular functions S_1 and S_2

D.1. The function $S_1[\theta, \phi, \Gamma_b]$

First, we consider the two functions

$$\begin{aligned} 1 - \vec{n} \cdot \vec{\beta}_0 &= 1 - \sqrt{1 - \Gamma_b^{-2}} \cos\theta - \frac{\sin\theta}{\Gamma_b} \frac{\cos\phi \varpi_x + \sin\phi \varpi_y}{E_0}, \\ 1 - \vec{n} \cdot \vec{\beta}_0 - \vec{n} \cdot \vec{\Delta\beta}_1 &= 1 - \sqrt{1 - \Gamma_b^{-2}} \cos\theta - \frac{\sin\theta}{\Gamma_b} \frac{\cos\phi(\varpi_x - z_a A_{\max}) + \sin\phi \varpi_y}{E_\perp[A_{\max}]}. \end{aligned} \tag{D.1}$$

Note that the latter has been derived from definitions (20*a*), (20*b*), (B.17) and (B.18). Thus, define

$$S_1[\theta, \Gamma_b, \Phi] = 1 - \sqrt{1 - \Gamma_b^{-2}} \cos\theta - \frac{\sin\theta}{\Gamma_b} \Phi[\phi, \varpi_x, \varpi_y, z_a A_{\max}], \tag{D.2}$$

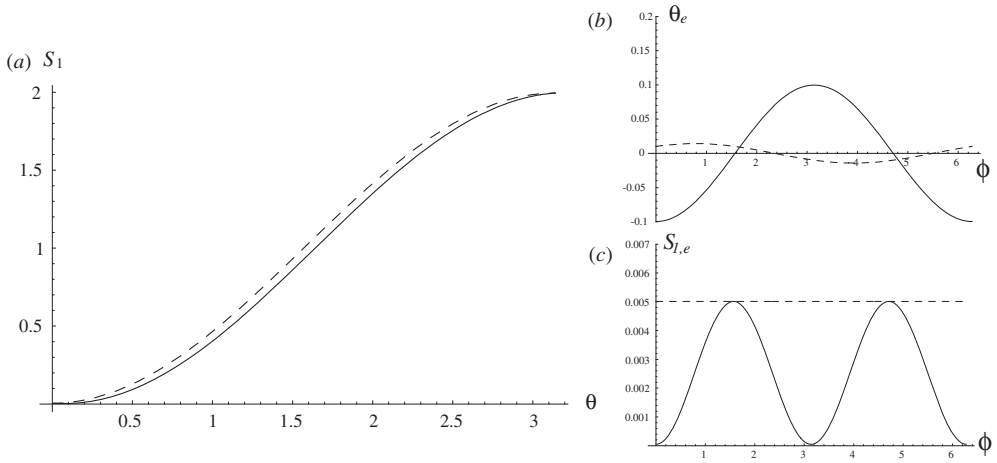

Figure D1. (*a*) Graph of the angular function $S_1[\theta, \Gamma_b = 10, \Phi]$ (39) with the standard parameters for Γ_b, $\varpi_{x,y}$ and $z_a A_{\max}$. Equation (D.1a) is shown as a dashed line here and in all subsequent plots, while equation (D.1b) is represented by a solid line. (*b*) Oscillation of the minimum angle θ_e (D.3) as a function of ϕ. The variation of equation (D.1a) is ten times magnified. (*c*) Minimum of the angular function S_1 (D.4) as a function of ϕ. Here, the variation of equation (D.1a) remains unchanged in amplitude and thus is nearly invisible.

with $|\Phi| < 1$ for all ϕ, ϖ_x, ϖ_y, $z_a A_{\max}$. S_1 is depicted in figure D1(*a*) and has extrema at

$$\theta_e = \arctan\left[\Phi\Big/\left(\Gamma_b^2 - 1\right)^{1/2}\right] + k\pi, \qquad k \in \mathbb{Z}, \tag{D.3}$$

with a minimum (for $k = 0$) at $\theta_e < \theta_{\max} \equiv \arctan\left[\left(\Gamma_b^2 - 1\right)^{-1/2}\right] = \arcsin\left[\Gamma_b^{-1}\right]$. This extremum leads (with $\Gamma_b \gg 1$) to

$$S_{1,e}[\theta_e, \Gamma_b, \Phi] = 1 \mp \sqrt{1 - \frac{1-\Phi^2}{\Gamma_b^2}} \simeq \begin{cases} (1-\Phi^2)\Big/\left(2\Gamma_b^2\right), \\ 2 - (1-\Phi^2)\Big/\left(2\Gamma_b^2\right), \end{cases} \tag{D.4}$$

where the upper sign is for even k and the lower sign for odd k. Note from equation (D.3) with $k = 0$ that the minimum of S_1 oscillates around zero. Second, the amplitude is limited by $S_{1,e}$. But as θ is constrained to $0 \leqslant \theta \leqslant \pi$, we have only one maximum for $\Phi < 0$ with $k = 1$ and one minimum for $\Phi > 0$ with $k = 0$. Variations of θ_e and $S_{1,e}$ are shown in figures D1(*b*), (*c*). However, note that $|\Phi| < 1$ always, so $S_1 > 0$.

D.2. The function $S_2[\theta, \phi, \Gamma_b]$

Here we have to consider the two functions

$$\begin{aligned} |\vec{n} \cdot \Delta\vec{\beta}_0| &= \frac{\sin\theta}{\Gamma_b} \frac{1}{4L^2(R')^2} \frac{\left|\sin\phi\varpi_x\varpi_y - \cos\phi\left(1+\varpi_y^2\right)\right|(z_a A_{\max})^3}{E_0^3}, \\ |\vec{n} \cdot \Delta\vec{\beta}_2| &= \frac{\sin\theta}{\Gamma_b} \frac{1}{4L^2} \frac{|\sin\phi\varpi_y|}{z_a A_{\max}}. \end{aligned} \tag{D.5}$$

Both functions are combined analogous to equation (40):

$$S_2[\theta, \Gamma_b, \Psi] = \frac{\sin\theta}{\Gamma_b} \Psi[\phi, \varpi_x, \varpi_y, z_a A_{\max}]. \tag{D.6}$$

Note that $\Psi \geqslant 0$ because of the absolute values in equations (D.5). S_2 has minima, $S_2 = 0$ for $\theta = 0, \pi$ or $\Psi = 0$. Furthermore, the maxima have the value $S_2[\theta = \pi/2] = \Psi/\Gamma_b$ as

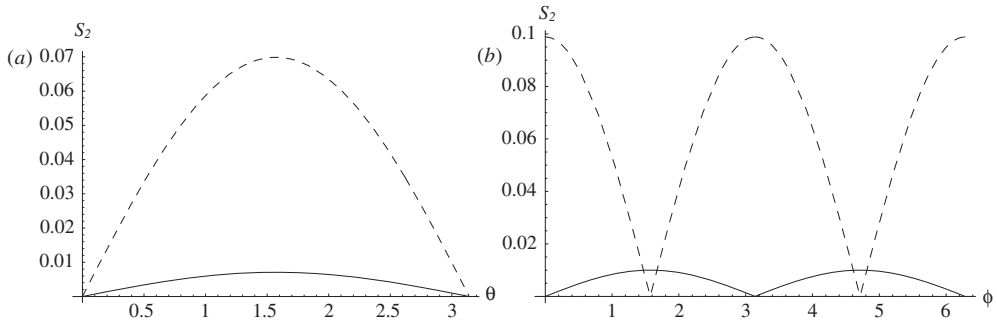

Figure D2. (*a*) Graph of the angular function $S_2[\theta, \Gamma_b = 10, \Psi](4L^2)$ (40) as a function of θ. Equation (D.5b) is shown as a solid line here and magnified by a factor of 10^2. (*b*) Graph of the angular function $S_2(4L^2)$ as a function of ϕ with $\theta = \pi/2$. Again, equation (D.5b) is magnified by a factor of 10^2. Thus, function (D.5a) is larger by about three orders of magnitude compared to factor (D.5b).

shown in figures D2(*a*), (*b*). Note that function (D.5a) for regime (a) is about 10^3 times larger than the counterpart in regime (b).

D.3. The ratio $S_r \equiv S_1/S_2$

The ratio

$$S_r = \frac{S_1}{S_2} = \frac{1 - \left(1 - \Gamma_b^{-2}\right)^{1/2} \cos\theta - (\sin\theta/\Gamma_b)\Phi}{(\sin\theta/\Gamma_b)\Psi} = \frac{\left[\Gamma_b - \left(\Gamma_b^2 - 1\right)^{1/2} \cos\theta\right] \Big/ \sin\theta - \Phi}{\Psi} \tag{D.7}$$

is important for further calculations and is shown in figure D3(*a*). Its properties will be derived in this subsection. The difference between the two solutions arise from the factor of magnitude 10^3 of the function S_2 for the two regimes. One finds that S_r has a minimum at

$$\theta_m = \arccos\left(1 - \Gamma_b^{-2}\right)^{1/2} = \arcsin\Gamma_b^{-1}, \tag{D.8}$$

independent of Φ or Ψ, and is depicted in figure D3(*b*). The matching minimum of S_r is given by

$$S_r[\theta_m, \Gamma_b] = (1 - \Phi)/\Psi, \tag{D.9}$$

independent of Γ_b. Note that, because $|\Phi| < 1$, $S_r > 0$ always. Again, clear differences between the two regimes are visible in figure D3(*c*).

Appendix E. The differential intensity spectrum for low frequencies $\omega \to 0$

Low frequencies $\omega \to 0$ lead to small parameters $\psi_{1,j}, |\psi_{3,j}| \to 0$. Thus, one can use the approximation (C.1),

$$M_n[\mathcal{A}_j; \psi_{1,j}, \psi_{3,j}] = \mathcal{A}_j^{n+1} \big/ (n+1), \tag{E.1}$$

to evaluate the integral (37) to lowest order in ω:

$$\begin{aligned} j_y &\simeq \Delta\beta_{0,y}(\zeta_{\text{end}} - \zeta_{\max})^3/3(\exp[-\mathrm{i}\omega l\zeta_{\text{end}}] + \exp[\mathrm{i}\omega l\zeta_{\text{end}} - \mathrm{i}\Delta\Phi(\zeta_{\text{end}})]) \\ &\quad + \left[\left(\Delta\beta_{1,y} - \Delta\beta_{2,y}\zeta_{\max}^2\right) 2\zeta_{\max} + 2\Delta\beta_{2,y}\zeta_{\max}(2\zeta_{\max})^2/2 - \Delta\beta_{2,y}(2\zeta_{\max})^3/3\right] \\ &\quad \times \exp[-\mathrm{i}\omega l\zeta_{\max} - \mathrm{i}\omega\Lambda(\vec{n}\cdot\Delta\vec{\beta}_0)(\zeta_{\text{end}} - \zeta_{\max})^3/3] \\ &\simeq 2\Delta\beta_{0,y}(\zeta_{\text{end}} - \zeta_{\max})^3/3 + 2\Delta\beta_{1,y}\zeta_{\max} - 2\Delta\beta_{2,y}\zeta_{\max}^3 \big/ 3 = \text{const}, \end{aligned} \tag{E.2}$$

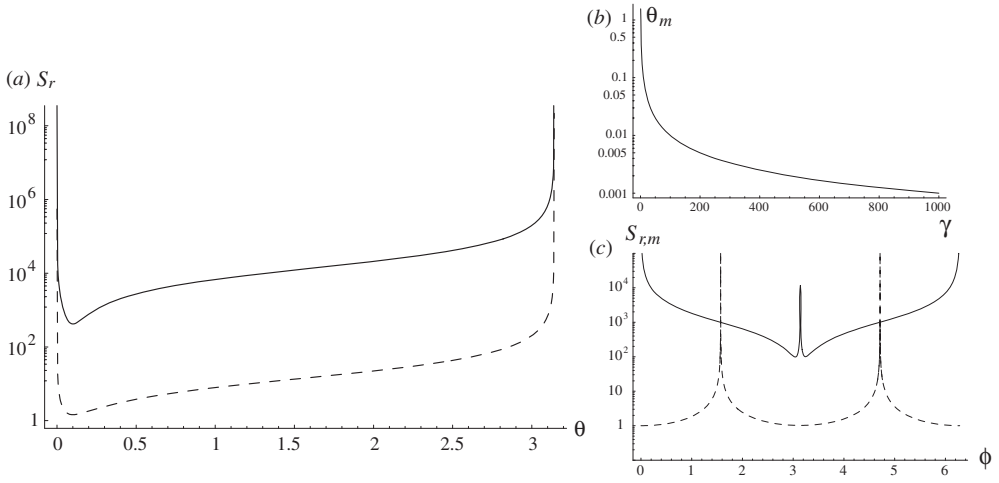

Figure D3. (*a*) Graph of the angular function $S_r[\theta, \Gamma_b = 10, \Phi, \Psi]/(4L^2) = S_1/[S_2(4L^2)]$. The difference between the two solutions arises from the function S_2. (*b*) The minimum angle θ_m (D.8) as a function of Γ_b. (*c*) Minimum of the angular function $S_r/(4L^2)$ from equation (D.9) as a function of ϕ.

with the phase factor (33) and in analogy

$$j_x \simeq 2\Delta\beta_{0,x}(\zeta_{\rm end} - \zeta_{\rm max})^3/3 + 2\Delta\beta_{1,x}\zeta_{\rm max} - 2\Delta\beta_{2,x}\zeta_{\rm max}^3/3 = \text{const}, \qquad \text{(E.3)}$$

with the subscript replacement.

Further, because $\zeta_{\rm end} = Lz_{\rm end}$ and $\zeta_{\rm max} = Lz_{\rm max}$ are functions of $R = R'/(z_a A_{\rm max})$, analytical approximations can be found:

$$z_{\rm max} \simeq 2(1-R) + (\pi/2)R^{8/7}, \qquad z_{\rm end} \simeq 2(1-R) + \pi R^{8/7}, \qquad \text{(E.4)}$$

leading to $z_{\rm end} - z_{\rm max} = (\pi/2)(R')^{8/7}/(z_a A_{\rm max})^{8/7}$ and $z_{\rm max} \simeq 2$ for $z_a A_{\rm max} \gg 1$. Using the approximations (B.23)–(B.30), one obtains to lowest order in $z_a A_{\rm max}$

$$j_x \simeq -\frac{2L}{\Gamma_b}(1 + B_x) \qquad j_y \simeq -\frac{2L}{\Gamma_b}B_y. \qquad \text{(E.5)}$$

With equations (A.23) and (A.24), one has

$$\vec{j}_\perp \cdot \vec{j}_\perp{}^* \simeq \frac{8L^2}{\Gamma_b^2}\begin{cases}\left[\dfrac{(\sin\phi - B_y)(1+B_x) - (\cos\phi - B_x)B_y}{1 - (\cos\phi B_x + \sin\phi B_y)}\right]^2 & \text{if} \quad 1/(2\Gamma_b) \leqslant \theta \leqslant 2/\Gamma_b \\ 1 + 2B_x + B_x^2 + B_y^2 & \text{otherwise}\end{cases}$$

$$\equiv \omega_0^{-2}/\Lambda^2 = \text{const}. \qquad \text{(E.6)}$$

Thus, the spectrum for one particle (remembering that $\Delta\Phi(\zeta_{\rm end})/\omega$ does not depend on ω; see equation (33)) is

$$\frac{{\rm d}^2 I}{{\rm d}\omega\,{\rm d}\Omega} \simeq \frac{e^2}{4\pi^2 c}\left(\frac{\omega}{\omega_0}\right)^2, \qquad \omega \ll \omega_{\rm low}, \qquad \text{(E.7)}$$

with

$$\omega_0 \simeq \frac{\Gamma_b}{2^{3/2}\Lambda L}\begin{cases}\left|\dfrac{1 - (\cos\phi B_x + \sin\phi B_y)}{(\sin\phi - B_y)(1+B_x) - (\cos\phi - B_x)B_y}\right| & \text{if} \quad 1/(2\Gamma_b) \leqslant \theta \leqslant 2/\Gamma_b \\ (1 + 2B_x + B_x^2 + B_y^2)^{-1/2} & \text{otherwise.}\end{cases} \qquad \text{(E.8)}$$

E.1. Calculation of the limiting frequency ω_{low}

From inequality (C.2), one has to find the frequency limit. Because there are two regimes (a) and (b), one has overall four terms that have to be considered:

$$\omega \ll \omega_{\text{low}} = \min[(\zeta_{c,j}/\mathcal{A}_j)\omega_{c,j}, 3(\zeta_{c,j}/\mathcal{A}_j)^3\omega_{c,j}] = (\zeta_{c,j}/\mathcal{A}_j)\omega_{c,j}\min[1, 3(\zeta_{c,j}/\mathcal{A}_j)^2]. \tag{E.9}$$

First, concentrate on the ratio

$$\Xi_j = 3\left(\frac{\zeta_{c,j}}{\mathcal{A}_j}\right)^2 \Big/ 1. \tag{E.10}$$

With $\zeta = zL$, one has for regime (b) with $z_a A_{\max}$ large

$$\Xi_b = \frac{3S_{r,b}}{4L^2 z_{\max}^2} \geqslant \frac{3S_{r,b}[\theta_m, \Gamma_b]}{16L^2} \simeq \frac{3}{4}\frac{z_a A_{\max}}{\varpi_y}\left|\frac{1+\cos\phi}{\sin\phi} - \frac{\varpi_y}{z_a A_{\max}}\right| \gg 1 \tag{E.11}$$

except in a region $\phi_* \simeq \pi$. A detailed calculation of the root in equation (E.11) yields

$$\phi_* \simeq 2\arctan\left[\frac{z_a A_{\max}/\varpi_y}{1 \pm 4/3}\right] \simeq \pi - 2\left(1 \pm \frac{4}{3}\right)\frac{\varpi_y}{z_a A_{\max}}. \tag{E.12}$$

Thus the regime $\Delta\phi$, where $\Xi_b < 1$, is

$$\Delta\phi \simeq \frac{16}{3}\frac{\varpi_y}{z_a A_{\max}} \to 0 \tag{E.13}$$

and so $\Xi_b \geqslant 1$ for almost all ϕ.

In regime (a), one has

$$\begin{aligned}\Xi_a &= \frac{3S_{r,a}}{L^2(z_{\text{end}} - z_{\max})^2} \\ &\simeq \frac{48}{\pi^2 (R')^{2/7}}(z_a A_{\max})^{-5/7} E_0^2 \left|\frac{E_0\left[\Gamma_b - \left(\Gamma_b^2 - 1\right)^{1/2}\cos\theta\right]/\sin\theta - (\cos\phi\varpi_x + \sin\phi\varpi_y)}{\sin\phi\varpi_x\varpi_y - \cos\phi\left(1+\varpi_y^2\right)}\right|.\end{aligned} \tag{E.14}$$

This expression has to be considered twice, first in the regime $\theta \simeq \arcsin\Gamma_b^{-1}$ where S_r has its minimum and outside otherwise. The first case yields (with $p_j \ll z_a A_{\max}$)

$$\begin{aligned}\Xi_a &\simeq \frac{48}{\pi^2 (R')^{2/7}}(z_a A_{\max})^{-5/7} E_0^2 \left|\frac{E_0 - (\cos\phi\varpi_x + \sin\phi\varpi_y)}{\sin\phi\varpi_x\varpi_y - \cos\phi\left(1+\varpi_y^2\right)}\right| \\ &\leqslant \frac{48}{\pi^2 (R')^{2/7}}(z_a A_{\max})^{-5/7}\frac{E_0^3}{\left|\sin\phi\varpi_x\varpi_y - \cos\phi\left(1+\varpi_y^2\right)\right|} < 1.\end{aligned} \tag{E.15}$$

However, equation (E.15) is fulfilled only if

$$\left|\sin\phi_*\varpi_x\varpi_y - \cos\phi_*\left(1+\varpi_y^2\right)\right| \geqslant \frac{48}{\pi^2 (R')^{2/7}}(z_a A_{\max})^{-5/7} E_0^3 \to 0. \tag{E.16}$$

The equality in equation (E.16) gives the root

$$\phi_0 \simeq \arctan\left[\frac{1+\varpi_y^2}{\varpi_x\varpi_y}\right] \tag{E.17}$$

and the boundaries of the constraint (E.15) can be obtained with the ansatz $\phi_* \simeq \phi_0 + \Delta\phi/2$ with $\Delta\phi \ll 1$ leading to

$$\Delta\phi \simeq \frac{96}{\pi^2 (R')^{2/7}} \underbrace{\frac{1+\varpi_x^2+\varpi_y^2}{\left(\left(1+\varpi_y^2\right)^2+\varpi_x^2\varpi_y^2\right)^{1/2}}}_{\mathcal{O}(1)} \underbrace{\frac{\left(1+\varpi_x^2+\varpi_y^2\right)^{1/2}}{z_a A_{\max}^{5/7}}}_{\ll 1} \to 0. \tag{E.18}$$

Thus, near $\theta \simeq \arcsin \Gamma_b^{-1}$ one has $\Xi_a < 1$ for almost all ϕ.

In the other case, the term of order Γ_b is the leading term in equation (E.14), with

$$\Xi_a \simeq \frac{48}{\pi^2 (R')^{2/7}} \frac{\Gamma_b}{(z_a A_{\max})^{5/7}} \underbrace{\frac{E_0^3}{\left|\sin\phi\varpi_x\varpi_y - \cos\phi\left(1+\varpi_y^2\right)\right|}}_{\geqslant 1} \underbrace{\frac{1-\left(1-\Gamma_b^{-2}\right)^{1/2}\cos\theta}{\sin\theta}}_{\geqslant 1}. \tag{E.19}$$

Thus, for $\Xi_a > 1$ one has the constraint

$$z_a A_{\max} < \left(\frac{48\Gamma_b}{\pi^2 (R')^{2/7}}\right)^{7/5} \simeq 9.16 \frac{\Gamma_b^{7/5}}{(R')^{2/5}}. \tag{E.20}$$

Because Γ_b is much greater than unity in astrophysical jets, equation (E.20) is fulfilled in the scenarios considered and therefore $\Xi_a > 1$. In combination, we have $\Xi_a < 1$ near $\theta \simeq \arcsin \Gamma_b^{-1}$ and $\Xi_a > 1$ elsewhere. In short, we approximate to first order that $\Xi_j > 1$ completely for regimes (a) and (b), and one has the constraint

$$\omega \ll \omega_{\text{low}} = (\zeta_{c,j}/\mathcal{A}_j)\omega_{c,j} = (\Lambda \mathcal{A}_j S_1)^{-1}. \tag{E.21}$$

Appendix F. The differential intensity spectrum for high frequencies $\omega \to \infty$

At first, one has to take into account that there are two different approximations of the functions $M_n^{\pm}[\mathcal{A}_j; \psi_{1,j}, \psi_{3,j}]$ of equation (37) as done in appendices C.2 and C.3. For $|\vec{n}\cdot\vec{\Delta\beta}_{0,2}| \simeq 0$ one has equation (C.11), whereas otherwise one has to use equations (C.7) and (C.10). Once exact formulae are given, one can distinguish at which angles one has to change the approximations.

F.1. Approximation of the functions $M_n^{\pm}[\mathcal{A}_j; \psi_{1,j}, \psi_{3,j}]$ for $|\vec{n}\cdot\vec{\Delta\beta}_{0,2}| \gg 0$

The first step is to approximate the functions $M_n^{\pm}[\mathcal{A}_j; \psi_{1,j}, \psi_{3,j}]$ of equation (37) in the manner of appendix C.2. In general, as mentioned before, there are two functional regimes for these M_n functions: (a) the outer regimes of the soliton (from $\pm\zeta_{\max}$ to $\pm\zeta_{\text{end}}$) with $\mathcal{A}_a = \zeta_{\text{end}} - \zeta_{\max}$, $\psi_{1,a} = \omega l$ and $\psi_{3,a} = -\omega\Lambda(\vec{n}\cdot\vec{\Delta\beta}_0)/3$; (b) the inner region (from $-\zeta_{\max}$ to $\zeta_{\max}$) with $\mathcal{A}_b = 2\zeta_{\max}$, $\psi_{1,b} = \omega(l - \Lambda(\vec{n}\cdot\vec{\Delta\beta}_1))$ and $\psi_{3,b} = \omega\Lambda(\vec{n}\cdot\vec{\Delta\beta}_2)/3$. Note that in both regimes, ψ_3 can be greater than or less than zero depending on whether $(\vec{n}\cdot\vec{\Delta\beta}_{0,2})$ is greater than or less than zero. One finds

$$\begin{aligned} &\sin\phi(\varpi_x\varpi_y) > \cos\phi\left(1+\varpi_y^2\right) && \text{for} \quad (\vec{n}\cdot\vec{\Delta\beta}_0) > 0, \\ &\sin\phi\varpi_y < -\cos\phi\left(1+\varpi_y^2\right)\big/(z_a A_{\max}) \to 0 && \text{for} \quad (\vec{n}\cdot\vec{\Delta\beta}_2) > 0, \end{aligned} \tag{F.1}$$

respectively. The two regions yield two different forms for the characteristic length and frequency:

$$\zeta_{c,a} \equiv \left(\frac{1-\vec{n}\cdot\vec{\beta}_0}{|\vec{n}\cdot\vec{\Delta\beta}_0|}\right)^{1/2} = S_{r,a}^{1/2}, \tag{F.2}$$

$$\zeta_{c,b} \equiv \left(\frac{1-\vec{n}\cdot\vec{\beta}_0-\vec{n}\cdot\Delta\vec{\beta}_1}{|\vec{n}\cdot\Delta\vec{\beta}_2|}\right)^{1/2} = S_{r,b}^{1/2}, \tag{F.3}$$

$$\omega_{c,a} \equiv \frac{1}{\Lambda}\left(\frac{|\vec{n}\cdot\Delta\vec{\beta}_0|}{(1-\vec{n}\cdot\vec{\beta}_0)^3}\right)^{1/2} = \frac{1}{\Lambda}\frac{1}{S_{1,a}S_{r,a}^{1/2}}, \tag{F.4}$$

$$\omega_{c,b} \equiv \frac{1}{\Lambda}\left(\frac{|\vec{n}\cdot\Delta\vec{\beta}_2|}{(1-\vec{n}\cdot\vec{\beta}_0-\vec{n}\cdot\Delta\vec{\beta}_1)^3}\right)^{1/2} = \frac{1}{\Lambda}\frac{1}{S_{1,b}S_{r,b}^{1/2}}. \tag{F.5}$$

Thus, one always has the approximations

$$M_n^+[\mathcal{A}_j;\psi_{1,j},\psi_{3,j}] \simeq \pi^{1/2}\psi_{1,j}^{-1/4+n/2}(3|\psi_{3,j}|)^{-1/4-n/2}\exp[-2k/3^{3/2}+\mathrm{i}n\pi/2], \tag{F.6}$$

$$M_n^-[\mathcal{A}_j;\psi_{1,j},\psi_{3,j}] \simeq \pi^{1/2}\psi_{1,j}^{-1/4+n/2}(3|\psi_{3,j}|)^{-1/4-n/2}\exp[2\mathrm{i}k/3^{3/2}-\mathrm{i}\pi/4]. \tag{F.7}$$

There are, then, two cases to consider: (1) for $(\vec{n}\cdot\Delta\vec{\beta}_{0,2}) > 0$ one has for region (a)

$$M_n^-[\mathcal{A}_a;\psi_{1,a},\psi_{3,a}] \simeq (\omega/\pi\omega_{c,a})^{-1/2}\zeta_{c,a}^{n+1}\exp[(2\mathrm{i}\omega/3\omega_{c,a})-\mathrm{i}\pi/4] \tag{F.8}$$

and for region (b)

$$M_n^+[\mathcal{A}_b;\psi_{1,b},\psi_{3,b}] \simeq (\omega/\pi\omega_{c,b})^{-1/2}\zeta_{c,b}^{n+1}\exp[-(2\omega/3\omega_{c,b})+\mathrm{i}n\pi/2]. \tag{F.9}$$

(2) For $(\vec{n}\cdot\Delta\vec{\beta}_{0,2}) < 0$, one obtains for regime (a)

$$M_n^+[\mathcal{A}_a;\psi_{1,a},\psi_{3,a}] \simeq (\omega/\pi\omega_{c,a})^{-1/2}\zeta_{c,a}^{n+1}\exp[-(2\omega/3\omega_{c,a})+\mathrm{i}n\pi/2] \tag{F.10}$$

and regime (b) simplifies to

$$M_n^-[\mathcal{A}_b;\psi_{1,b},\psi_{3,b}] \simeq (\omega/\pi\omega_{c,b})^{-1/2}\zeta_{c,b}^{n+1}\exp[\mathrm{i}(2\omega/3\omega_{c,b})+\mathrm{i}\pi/4]. \tag{F.11}$$

Because of the need to satisfy inequality (C.8), one finds that M_n^- is negligible when

$$\zeta_{c,j}^2 > \mathcal{A}_j^2 \quad \Leftrightarrow \quad (\zeta_{c,j}/\mathcal{A}_j)^2 > 1. \tag{F.12}$$

This ratio differs from the ratio (E.10) only by a factor of 3. Because one had the result that $\Xi_j \gg 1$ practically for all cases one can apply the result from appendix E.1 here to separate the considerations. Mostly, M_n^- can be neglected except for $\theta \simeq \arcsin\Gamma_b^{-1}$ where $\Xi_a \leqslant 1$. Here, the integrals M_n^- apply, which has no damping exponential term for high frequencies. This case is considered subsequently in this paper.

F.2. Solution for high frequencies

With the phase factor

$$1/\Omega \equiv l\zeta_{\max} + \Lambda(\vec{n}\cdot\Delta\vec{\beta}_0)(\zeta_{\mathrm{end}}-\zeta_{\max})^3/3 \tag{F.13}$$

and the definition

$$\zeta_{b,y} \equiv \left(\Delta\beta_{1,y}-\Delta\beta_{2,y}\zeta_{\max}^2\right)\zeta_{c,b} + 2\mathrm{i}\Delta\beta_{2,y}\zeta_{\max}\zeta_{c,b}^2 + \Delta\beta_{2,y}\zeta_{c,b}^3, \tag{F.14}$$

one has for j_y, by neglecting all M_n^- and for case (1)

$$j_y \simeq \zeta_{b,y}(\omega/\pi\omega_{c,b})^{-1/2}\exp[-(2\omega/3\omega_{c,b})-\mathrm{i}\omega/\Omega], \tag{F.15}$$

containing only terms of regime (b). The other case (2) is given by

$$j_y \simeq -2\Delta\beta_{0,y}(\omega/\pi\omega_{c,a})^{-1/2}\zeta_{c,a}^3\exp[-(2\omega/3\omega_{c,a})-\mathrm{i}\Delta\Phi(\zeta_{\mathrm{end}})/2]$$
$$\times\cos[-\omega l\zeta_{\mathrm{end}}+\Delta\Phi(\zeta_{\mathrm{end}})/2] \tag{F.16}$$

and has only terms of regime (a). Note that j_x can be treated in analogy. Now one maintains only the terms of leading order in $z_a A_{\max}$ (in the parameters $\Delta\beta$, ζ_c and ω_c). One finds that in regime (b) one has terms with $(z_a A_{\max})^{1/4}$, whereas in regime (a) the leading term is of order $(z_a A_{\max})^{-3/4}$. Thus, one can concentrate on regime (b) and case (1) yielding

$$\begin{aligned} j_x &\simeq \Delta\beta_{1,x}\zeta_{c,b}(\omega/\pi\omega_{c,b})^{-1/2}\exp[-(2\omega/3\omega_{c,b}) - \mathrm{i}\omega/\Omega], \\ j_y &\simeq \left(\Delta\beta_{1,y}\zeta_{c,b} + \Delta\beta_{2,y}\zeta_{c,b}^3\right)(\omega/\pi\omega_{c,b})^{-1/2}\exp[-(2\omega/3\omega_{c,b}) - \mathrm{i}\omega/\Omega]. \end{aligned} \tag{F.17}$$

In each term of equation (A.16), there emerge the products of $j_{x,y}$ and $j_{x,y}^*$, namely

$$\begin{aligned} |j_x|^2 &\simeq \pi\Delta\beta_{1,x}^2\zeta_{c,b}^2\omega_{c,b}\exp[-(4\omega/3\omega_{c,b})]/\omega, \\ |j_y|^2 &\simeq \pi\left(\Delta\beta_{1,y}\zeta_{c,b} + \Delta\beta_{2,y}\zeta_{c,b}^3\right)^2\omega_{c,b}\exp[-(4\omega/3\omega_{c,b})]/\omega. \end{aligned} \tag{F.18}$$

Because in this part the neighborhood of $\theta = \arcsin\Gamma_b^{-1} \simeq \Gamma_b^{-1}$ is omitted, one can use equation (A.23) for equation (A.16) leading to

$$\Lambda^2\vec{j}_\perp\cdot\vec{j}_\perp^{\,*} = (\omega/\pi\omega_{c,b})^{-1}\omega_B^{-2}\exp[-(4\omega/3\omega_{c,b})], \tag{F.19}$$

where

$$\omega_B^{-2} \equiv \Lambda^2\left[\Delta\beta_{1,x}^2 + \left(\Delta\beta_{1,y} + \Delta\beta_{2,y}\zeta_{c,b}^2\right)^2\right]\zeta_{c,b}^2. \tag{F.20}$$

This solution can be simplified to

$$\begin{aligned} \omega_B &= \frac{1}{\Lambda}\left(\frac{S_2}{S_1^3}\right)^{1/2}\left[\left(\frac{1}{\sin\theta\sin\phi} + \frac{1}{\Gamma_b S_1}\frac{\varpi_y}{E_0}\right)^2 + \frac{1}{\Gamma_b S_1}\left(1+\frac{\varpi_x}{E_0}\right)^2\right]^{-1/2} \\ &= \omega_{c,b}\left[\left(\frac{1}{\sin\theta\sin\phi} + \frac{1}{\Gamma_b S_1}\frac{\varpi_y}{E_0}\right)^2 + \frac{1}{\Gamma_b^2 S_1^2}\left(1+\frac{\varpi_x}{E_0}\right)^2\right]^{-1/2}. \end{aligned} \tag{F.21}$$

Thus, the spectrum for one particle is in the leading case (1) and regime (b):

$$\frac{\mathrm{d}^2 I}{\mathrm{d}\omega\,\mathrm{d}\Omega} \simeq \frac{e^2}{4\pi^2 c}\left[\left(\frac{1}{\sin\theta\sin\phi} + \frac{1}{\Gamma_b S_1}\frac{\varpi_y}{E_0}\right)^2 + \frac{1}{\Gamma_b^2 S_1^2}\left(1+\frac{\varpi_x}{E_0}\right)^2\right]\frac{\pi\omega}{\omega_{c,b}}\exp[-(4\omega/3\omega_{c,b})] \tag{F.22}$$

and afar from the minimum of S_1 (at $\theta \simeq \arcsin\Gamma_b^{-1}$), one can approximate

$$\frac{\mathrm{d}^2 I}{\mathrm{d}\omega\,\mathrm{d}\Omega} \simeq \frac{e^2}{4\pi^2 c}\frac{\pi\omega}{\omega_{c,b}\sin^2\theta\sin^2\phi}\exp[-(4\omega/3\omega_{c,b})]. \tag{F.23}$$

Now returning to the case with $\theta \simeq \arcsin\Gamma_b^{-1}$, one has to basically consider M_n^- of regime (a) and case (1) due to appendix E.1. This approximation leads to

$$\begin{aligned} j_y \simeq{}& 2\Delta\beta_{0,y}(\omega/\pi\omega_{c,a})^{-1/2}\zeta_{c,a}^3\exp[-\mathrm{i}\Delta\Phi(\zeta_{\mathrm{end}})/2] \\ &\times\cos[-(2\omega/3\omega_{c,a}) - \omega l\zeta_{\mathrm{end}} + \Delta\Phi(\zeta_{\mathrm{end}})/2 - \pi/4], \end{aligned} \tag{F.24}$$

and j_x is obtained in analogy. Again, the products of $j_{x,y}$ and $j_{x,y}^*$ have to be calculated for equation (A.16), yielding (after averaging over the $\cos^2$ terms)

$$\begin{aligned} |j_x|^2 &\simeq 2\pi\Delta\beta_{0,x}^2\zeta_{c,a}^6\omega_{c,a}/\omega, \\ |j_x j_y^*| &\simeq 2\pi\Delta\beta_{0,x}\Delta\beta_{0,y}\zeta_{c,a}^6\omega_{c,a}/\omega, \\ |j_y|^2 &\simeq 2\pi\Delta\beta_{0,y}^2\zeta_{c,a}^6\omega_{c,a}/\omega. \end{aligned} \tag{F.25}$$

Because equation (A.24) is valid, one has as a result

$$\Lambda^2|\vec{j}_\perp|^2 = (\omega/\pi\omega_{c,a})^{-1}\omega_A^{-2}, \tag{F.26}$$

where

$$\omega_A^{-2} \equiv 2\Lambda^2 \left(\frac{(\sin\phi - B_y)\Delta\beta_{0,x} - (\cos\phi - B_x)\Delta\beta_{0,y}}{1 - (\cos\phi B_x + \sin\phi B_y)} \right)^2 \zeta_{c,a}^6. \tag{F.27}$$

This result can be simplified to

$$\begin{aligned}\omega_A &= \frac{1}{\Lambda}\left(\frac{S_2}{S_1^3}\right)^{1/2} \frac{\sin\theta|\sin\phi|}{2^{1/2}} \frac{|\sin\phi\varpi_x\varpi_y - \cos\phi\left(1+\varpi_y^2\right)|(1 - (\cos\phi B_x + \sin\phi B_y))}{|(\sin\phi - B_y)\left(1+\varpi_y^2\right) - (\cos\phi - B_x)\varpi_x\varpi_y|} \\ &\simeq \omega_{c,a}\frac{|\cos\phi|}{2^{1/2}\Gamma_b},\end{aligned} \tag{F.28}$$

leading to the result

$$\frac{\mathrm{d}^2 I}{\mathrm{d}\omega\,\mathrm{d}\Omega} \simeq \frac{e^2}{4\pi^2 c}\frac{2\pi\Gamma_b^2\omega}{\omega_{c,a}\cos^2\phi}. \tag{F.29}$$

F.3. Calculation of the limiting frequency ω_{high}

Similar to the case for low frequencies, one has to investigate the condition

$$\omega_{\mathrm{high}} = \max\{(\zeta_{c,j}/\mathcal{A}_j)\omega_{c,j}, 3(\zeta_{c,j}/\mathcal{A}_j)^3\omega_{c,j}\} = (\zeta_{c,j}/\mathcal{A}_j)\omega_{c,j}\max\{1, 3(\zeta_{c,j}/\mathcal{A}_j)^2\}, \tag{F.30}$$

with the same ratio $\Xi_j = 3(\zeta_{c,j}/\mathcal{A}_j)^2$. Because it is known that $\Xi_j > 1$ except for $\theta \simeq \Gamma_b^{-1}$, one has for equation (F.23)

$$\omega \gg \omega_{\mathrm{high}} = 3(\zeta_{c,b}/\mathcal{A}_b)^3\omega_{c,b} = 3\big/\left(\Lambda\mathcal{A}_b^3 S_{2,b}\right). \tag{F.31}$$

First, note that ω_{high} could increase to infinity, but only for $|n_y| \to 0$. However, this behavior corresponds with $|\vec{n}\cdot\Delta\vec{\beta}_2| \to 0$, and then the original approximation of appendix C.2 is not valid. Then one has to turn to the approximation of appendix C.3, which is done subsequently. For equation (F.29), one finds

$$\omega \gg \omega_{\mathrm{high}} = (\zeta_{c,a}/\mathcal{A}_a)\omega_{c,j} = (\Lambda\mathcal{A}_a S_{1,a})^{-1}. \tag{F.32}$$

F.4. Approximation of the functions $M_n^{\pm}[\mathcal{A}_j; \psi_{1,j}, \psi_{3,j}]$ *for* $|\vec{n}\cdot\vec{\Delta}\beta_{0,2}| \simeq 0$

First, one has to calculate the angular region $\Delta\phi$ given by

$$3\left(\frac{\zeta_{c,j}}{\mathcal{A}_j}\right)^3\omega_{c,j} = \frac{\omega\Lambda S_2}{3}\mathcal{A}_j^3 \ll 1. \tag{F.33}$$

Thus, one can estimate the conditions for regimes (a) and (b):

$$\begin{aligned}&\left|\sin\phi_{*,a}\varpi_x\varpi_y - \cos\phi_{*,a}\left(1+\varpi_y^2\right)\right| \ll \frac{96}{\pi^3(R')^{10/7}}\frac{\Gamma_b}{\sin\theta}E_0^3(z_a A_{\max})^{3/7}\frac{1}{\omega(\Lambda L)}, \\ &|\sin\phi_{*,b}\varpi_y| \ll \frac{3}{16}\frac{\Gamma_b}{\sin\theta}z_a A_{\max}\frac{1}{\omega(\Lambda L)}.\end{aligned} \tag{F.34}$$

Assuming that $\varpi_j \ll 1$ in the first regime, the angular regions $\Delta\phi$ are in the neighborhood of $\pi/2$ and $3\pi/2$ in regime (a) and near $0, \pi, 2\pi$ in regime (b). Note that for any electron, there exists a frequency so that the right-hand side is small where one can estimate

$$\begin{aligned}\Delta\phi_a &\ll \frac{192}{\pi^3(R')^{10/7}}\frac{\Gamma_b}{\sin\theta}(z_a A_{\max})^{3/7}\frac{1}{\omega(\Lambda L)}, \\ \Delta\phi_b &\ll \frac{3}{8}\frac{\Gamma_b}{\sin\theta}\frac{z_a A_{\max}}{\varpi_y}\frac{1}{\omega(\Lambda L)}.\end{aligned} \tag{F.35}$$

The procedure for the spectrum (applying approximation (C.11)) is similar to the previous subsection. However, this time the terms $j_{x,y}$ are of order $(z_a A_{\max})^{5/7}$ in regime (a) and only of order 1 in regime (b). Thus, one has

$$j_y \simeq -\frac{2\Delta\beta_{0,y}(\zeta_{\rm end}-\zeta_{\max})^2}{\omega\Lambda(1-\vec{n}\cdot\vec{\beta}_0)}\sin[\omega\Lambda\zeta_{\max}(1-\vec{n}\cdot\vec{\beta}_0-\vec{n}\cdot\Delta\vec{\beta}_1)]\exp[{\rm i}\omega\Lambda\zeta_{\max}(\vec{n}\cdot\Delta\vec{\beta}_1)], \tag{F.36}$$

and j_x analogously. For the products $|j_{x,y}|^2$, the $\sin^2$ components can be averaged due to the large frequencies yielding

$$\begin{aligned} |j_x|^2 &\simeq \frac{2\Delta\beta_{0,x}^2(\zeta_{\rm end}-\zeta_{\max})^4}{\Lambda^2(1-\vec{n}\cdot\vec{\beta}_0)^2\omega^2},\\ |j_x j_y^*|^2 &\simeq \frac{2\Delta\beta_{0,x}\Delta\beta_{0,y}(\zeta_{\rm end}-\zeta_{\max})^4}{\Lambda^2(1-\vec{n}\cdot\vec{\beta}_0)^2\omega^2},\\ |j_y|^2 &\simeq \frac{2\Delta\beta_{0,y}^2(\zeta_{\rm end}-\zeta_{\max})^4}{\Lambda^2(1-\vec{n}\cdot\vec{\beta}_0)^2\omega^2}. \end{aligned} \tag{F.37}$$

Thus, one has

$$\Lambda^2\vec{j}_\perp\cdot\vec{j}_\perp{}^* \simeq \alpha^2/\omega^2, \tag{F.38}$$

with, using $1+\varpi_y^2 = E_0^2(1-B_x^2)$,

$$\alpha^2 \simeq \frac{\pi^4(R')^{4/7}(z_a A_{\max})^{10/7}}{128\Gamma_b^2 S_{1,a}^2 E_0^2}\begin{cases}\left[\frac{(\sin\phi-B_y)(1-B_x^2)-(\cos\phi-B_x)B_xB_y}{1-(\cos\phi B_x+\sin\phi B_y)}\right]^2 & \text{if}\quad 1/(2\Gamma_b)\leqslant\theta\leqslant 2/\Gamma_b\\ 1-2B_x^2+B_x^4+B_x^2B_y^2 & \text{otherwise}\end{cases} \tag{F.39}$$

and finally for $|\vec{n}\cdot\Delta\vec{\beta}_{0,2}|\simeq 0$,

$$\frac{{\rm d}^2 I}{{\rm d}\omega\,{\rm d}\Omega} \simeq \frac{e^2\omega^2}{4\pi^2 c}\frac{\alpha^2}{\omega^2} = \frac{e^2\alpha^2}{4\pi^2 c} = \text{const.} \tag{F.40}$$

F.5. Calculation of the limiting frequency for equation (F.40)

The last task here is to find the proper lower limit for the validity of the approximation (C.11). From inequality (C.12), one obtains the same limit $\omega^*_{\rm high}$ as given in equation (F.32):

$$\omega \gg \omega^*_{\rm high} \simeq (\Lambda\mathcal{A}_a S_{1,a})^{-1}. \tag{F.41}$$

References

[1] Klebesadel R W, Strong I B and Olson R A 1973 *Astrophys. J.* **182** L85
[2] Hurley K 1986 *Gamma-ray Burst and Neutrino Star Physics (AIP Conf. Proc. 141)* ed E P Liang and V Petrosian (New York: AIP) chapter 1
[3] Meegan C A *et al* 1992 *Nature* **290** 378
[4] Fishman G J and Meegan C A 1995 *Annu. Rev. Astron. Astrophys.* **33** 415
[5] Briggs M S *et al* 1996 *Astrophys. J.* **451** 40
[6] McNamaram B J, Harrison T E and Wiliams C L 1995 *Astrophys. J.* **452** L25
[7] Frail D A and Kulkarni S R 1995 *Astrophys. Space Sci.* **231** 277
[8] van Paradijs J *et al* 1997 *Nature* **386** 686
[9] Frail D A, Kulkarni S R, Nicastro L, Feroci M and Taylor G B 1997 *Nature* **389** 261
[10] Metzger M *et al* 1997 *Nature* **387** 878

[11] Kulkarni S R *et al* 1999 *Gamma-Ray Bursts (AIP Conf. Proc. 526)* ed M Kippen, R Mallozzi and G Fishman (New York: AIP) p 277
[12] Schlickeiser R, Vainio R, Böttcher M, Lerche I, Pohl M and Schuster C 2002 *Astron. Astrophys.* **393** 69–87
[13] Piran T 1999 *Phys. Rep.* **314** 575
[14] van Paradijs J, Kouveliotou C and Wijers R A M J 2000 *Annu. Rev. Astron. Astrophys.* **38** 379
[15] Mészáros P 2002 *Annu. Rev. Astron. Astrophys.* **40** 137
[16] Piran T 2005 *Rev. Mod. Phys.* **76** 1143
[17] Schaefer-Rolffs U and Lerche I 2006 *Phys. Plasmas* **12** 062303
[18] Jackson J D 1962, 1975 *Classical Electrodynamics* 2nd edn (New York: Wiley)
[19] Weibel E S 1959 *Phys. Rev. Lett.* **2** 83
[20] Fried B D 1959 *Phys. Fluids* **2** 337
[21] Brainerd J J 2000 *Astrophys. J.* **538** 628
[22] Achterberg A, Wiersma J and Norman C A 2007 *Astron. Astrophys.* **475** 19–36
[23] Tautz R C and Lerche I 2006 *Astrophys. J.* **653** 447
[24] Medvedev M V and Loeb A 1999 *Astrophys. J.* **526** 697
[25] Medvedev M V 2007 *Astrophys. Space Sci.* **307** 245
[26] Medvedev M V, Lazzati D, Morsony B C and Workman J C 2007 *Astrophys. J.* **666** 339